

Two-Photon Mechanism of Particle Production by High-Energy Colliding Beams*

Stanley J. Brodsky

Stanford Linear Accelerator Center, Stanford, California 94305

and

Toichiro Kinoshita and Hidezumi Terazawa†

Laboratory of Nuclear Studies, Cornell University, Ithaca, New York 14850

(Received 3 May 1971)

We report on the calculation of the cross sections for the production of positive-charge-conjugation states such as π^0 , η , e^+e^- , $\mu^+\mu^-$, and $\pi^+\pi^-$ by a two-photon mechanism in e^-e^+ and e^-e^- collisions. We give the precise relationship of the process $e+e\rightarrow e+e+X$ (X is any $C=+$ state) to the corresponding two-photon annihilation process $\gamma+\gamma\rightarrow X$, as well as a careful derivation of the equivalent-photon approximation. In the case of the π^0 production, we have found that, for the beam energy E in the 1–3 GeV range, the exact total cross section is 20–30% larger than the one calculated previously in the equivalent-photon approximation. However, the introduction of form factors cuts down the exact total cross section, reducing it to within 10% of the equivalent-photon-approximation result. For η production the agreement is even better. Thus it appears that the use of the equivalent-photon approximation is justified in most cases. We discuss detailed angular distributions in this approximation for the case of $\pi^+\pi^-$ production. One important problem which cannot be adequately studied in the equivalent-photon approximation is the degree of noncoplanarity of the $\pi^+\pi^-$ (and the $\mu^+\mu^-$) pair. We have studied this problem using the exact formula and found that, for $E=1$ GeV, typically 40–50% of pion pairs will be produced with the noncoplanarity angle greater than 12° . We discuss the general structure of the $\gamma+\gamma\rightarrow\pi^++\pi^-$ amplitude as well as a simple model incorporating the σ meson. We also give a rough estimate of multi-hadron production cross sections.

I. INTRODUCTION

The importance of the two-photon mechanism of lepton and hadron production in electron-positron (or electron-electron¹) colliding-beam experiments at high energies has been recently emphasized by several groups.^{2–4} By the two-photon mechanism we mean the process of the type

$$e+e\rightarrow e+\gamma^*+e+\gamma^*\rightarrow e+e+X, \quad (1.1)$$

in which electrons of both incident beams emit virtual (spacelike) photons (γ^* 's) which in turn annihilate, producing a final state X , where X may be a lepton state such as e^+e^- , $\mu^+\mu^-$, or any possible neutral $C=+$ hadron state such as $\pi^+\pi^-$, $\pi^+\pi^-\pi^0$, π^0 , η , K^+K^- , etc. [see Fig. 1(a)]. The cross section for the process (1.1) is obviously of order α^4 and is completely negligible at low beam energies (up to several hundred MeV) compared with the cross section for the more familiar "one-photon" or " e^+e^- -annihilation" mechanism

$$e^++e^-\rightarrow\gamma^*\rightarrow\pi^++\pi^-, \text{ etc.}, \quad (1.2)$$

which is of order α^2 .

However, as the beam energy increases, two factors operate to reverse the relative importance of these two mechanisms: (1) Whereas the cross section for the one-photon process (1.2) will even-

tually decrease with the beam energy as $\sim E^{-2}$,⁵ this energy factor is replaced in the cross section for (1.1) by a constant m^{-2} (where m is usually the threshold mass of the state X). This is an example of the circumstance pointed out by Cheng and Wu⁶ in which the asymptotic behavior of higher-order terms may be completely different from that of lower-order terms. (2) In the process (1.1) both incident particles are electrons which radiate photons so readily that the corresponding cross section is enhanced by two factors of $\ln(E/m_e)$ ($\simeq 7.6$ for $E=1$ GeV), in addition to other possible logarithmic terms which can be inferred from the Cheng-Wu analysis of massive-photon quantum electrodynamics. For these reasons, the two-photon cross section for (1.1) is found to behave asymptotically as

$$\sigma(E) \propto \frac{\alpha^4}{m^2} \left(\ln \frac{E}{m_e} \right)^2 \left(\ln \frac{E}{m} \right)^n, \quad (1.3)$$

where n is a real number ≥ 1 which depends on the high-energy behavior of the cross section $\sigma_{\gamma\gamma\rightarrow X}$. In the case $X=\pi^+\pi^-$, this cross section becomes comparable with the one-photon cross section ($\sigma \propto \alpha^2 E^{-2}$) at an energy per beam $E \simeq 1.5$ GeV,⁷ even if we treat pions as pointlike. For higher energies the two-photon process becomes clearly the dominant one. This means, on one hand, that

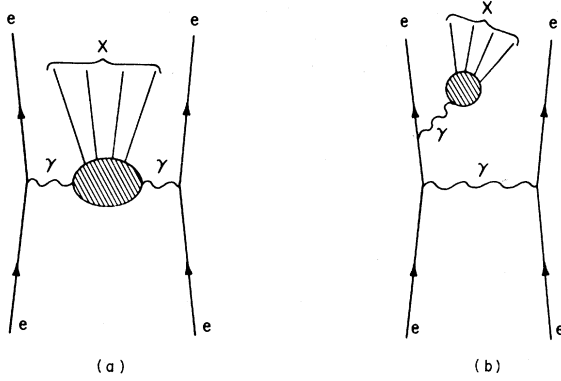


FIG. 1. Colliding-beam production of (a) neutral $C=+$ state and (b) neutral $C=-$ state. In the case of the e^-e^+ collision, there are also diagrams in which the initial e^- and e^+ annihilate each other and a new e^-e^+ pair is created in the final state. These Bhabha-type amplitudes are omitted throughout this paper because their contributions are quite small.

the magnitude of the two-photon cross sections at high energy is large enough to open the way to a complete exploration of the photon-photon annihilation process including the $C=+$ hadron resonances. On the other hand, these hadrons would also form a serious background to other processes of interest, especially the one-photon annihilation process (1.2), and make these experiments more difficult. In any case, in order to be able to extract interesting physics from the high-energy colliding-beam experiments, it is imperative to understand not only the qualitative but also the quantitative characteristics of the two-photon cross sections.⁸

Theoretical investigation of the two-photon mechanism goes back to 1934 when Williams and Landau and Lifshitz⁹ studied the production of electron-positron pairs by this mechanism. Around 1960 when the colliding-beam facilities were about to become available,¹⁰ the two-photon mechanism

caught some attention. Calogero and Zemach¹¹ studied the pion pair production in electron-electron collisions. Low¹² calculated the cross section for π^0 production by colliding electrons, which he proposed as a means of measuring the π^0 lifetime. In his paper the $[\ln(E/m_e)]^2 \ln(E/m_\pi)$ energy dependence of the two-photon cross section is clearly evident. For nearly ten years afterwards, however, the two-photon mechanism attracted little attention. This is because the energies available at the existing colliding-beam facilities were too low for this mechanism to be important and attention was focused solely on the production of $C=-$ resonances by the e^+e^- -annihilation mechanism (1.2).

As the beam energy has steadily increased and new data have begun to be reported,¹³ however, the two-photon mechanism has again become a subject of intense investigation. DeCelles and Goehl¹⁴ have studied some aspects of the process (1.1) for σ production in order to explore the feasibility of experimental determination of S -wave $\pi\pi$ phase shifts. More recently, Arteaga-Romero *et al.*³ have calculated the two-photon cross sections for $\mu^+\mu^-$, $\pi^+\pi^-$, and K^+K^- production at $E=2$ and 3 GeV, and pointed out that these cross sections are rather large and increase with beam energy. Independently, Budnev *et al.*⁴ and our group² have also investigated the two-photon mechanism. We have paid particular attention to detailed features such as angular distribution, angular correlation, and mass distribution of produced hadrons which would help us to distinguish the two-photon process from the one-photon process.

In all these works on the two-photon mechanism,²⁻⁴ calculations have been carried out in the equivalent-photon approximation,^{15,16} which is useful for understanding the main qualitative features. In this approximation, the leading behavior for $m_e/E \rightarrow 0$ of the cross section for the process (1.1) when the final electrons are not detected is given by (see Fig. 2 for notation)

$$d\sigma_{ee \rightarrow eeX}(E) \cong \left(\frac{2\alpha}{\pi}\right)^2 \left(\ln \frac{E}{m_e}\right)^2 \int \frac{d\omega_1}{\omega_1} \frac{d\omega_2}{\omega_2} \frac{(E^2 + E_1'^2)(E^2 + E_2'^2)}{4E^4} d\sigma_{\gamma\gamma \rightarrow X}(\omega_1, \omega_2), \quad (1.4)$$

where $d\sigma_{\gamma\gamma \rightarrow X}$ is the differential cross section for the annihilation of two oppositely directed real unpolarized photons of energy ω_1 and ω_2 into a state X . For the total cross section, noting that $\sigma_{\gamma\gamma \rightarrow X}$ is a function of $s = (k_1 + k_2)^2 \cong 4\omega_1\omega_2$ only, we obtain

$$\sigma_{ee \rightarrow eeX}(E) \cong 2 \left(\frac{\alpha}{\pi}\right)^2 \left(\ln \frac{E}{m_e}\right)^2 \int_0^{4E^2} \frac{ds}{s} f\left(\frac{\sqrt{s}}{2E}\right) \sigma_{\gamma\gamma \rightarrow X}(s), \quad (1.5)$$

as in Low's work,¹² where $f(\sqrt{s}/2E)$ is given by

(3.4). Substitution of the explicit form of the cross section, for example,

$$\sigma_{\gamma\gamma \rightarrow X} \sim (\ln s)^{n'}, \quad (1.6)$$

where n' depends on the state X , leads to the result of the form (1.3) with $n = n' + 2$ if $n' \geq -1$ and $n = 1$ if $n' < -1$.

During the last year it has thus been qualitatively established that the two-photon mechanism becomes the dominant process in colliding-beam experi-

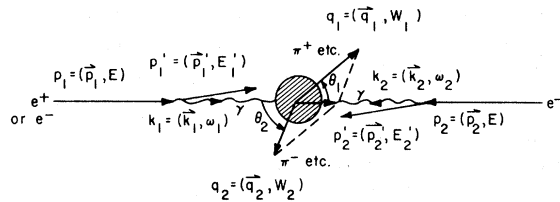


FIG. 2. Kinematics and notation for the pair production of various particles by two-photon mechanism.

ments as the beam energy increases above ~ 1 GeV. We are now entering the stage in which more quantitative knowledge of this process is required. From this point of view previous results are not completely satisfactory because they have all been obtained by means of the equivalent-photon approximation or its variants. Although this approximation will give the leading logarithmic E/m_e dependence of the cross section, the reliability of the method at usual laboratory energies has not been established. One of the purposes of this paper is to investigate this question closely and find out how good this approximation actually is.

In Sec. II we give a convenient formula for the cross section for the production of $C = +$ states by the two-photon mechanism. Aside from the approximation in which we omit the Møller (or Bhabha) interference term and ignore, whenever it is safe, the electron mass m_e in comparison with the electron energy E , this α^4 formula is exact and can be used as the starting point of further calculations. The effect of interference in e^-e^- collisions is clearly negligible, since the probability for both incident electrons to scatter backwards is very small. In Sec. III we show how the cross sections in the equivalent-photon approximation can be derived from the result of Sec. II. Next, we examine in Sec. IV the accuracy of the equivalent-photon approximation in the particularly simple case of π^0 and η production, by calculating these cross sections in both exact and approximate ways. This has led us to a conclusion that the equivalent-photon approximation is in fact fairly reliable (better than 30% accuracy). Based on this information we study in Sec. V the production of $\pi^+\pi^-$ and $\mu^+\mu^-$ pairs in detail in the equivalent-photon approximation. We discuss in Sec. VI the general structure of the $\gamma + \gamma \rightarrow \pi + \pi$ amplitude, and give a simple illustration of hadronic modification due to the σ enhancement. One important problem which cannot be adequately studied in the equivalent-photon approximation is the degree of noncoplanarity of the $\pi^+\pi^-$ pair. We investigate this problem in Sec. VII using the exact formula obtained in Sec. II, and determine the degree of noncoplanarity numerically. Section VIII is devoted to the discussion of various

related problems. A review of formulas obtained by the equivalent-photon approximation of Dalitz and Yennie is given in the Appendix.

II. TWO-PHOTON CROSS SECTION FOR PARTICLE PRODUCTION

Diagrams of the type shown in Figs. 1(a) and 1(b) both contribute to the process $e^+e^- \rightarrow e^+e^-X$. In this paper, however, we shall concentrate on the diagrams of the first kind (two-photon diagrams) because (1) the diagrams of the second kind will have fewer factors of $\ln(E/m_e)$, (2) the contributions of the first ($C = +$) and second ($C = -$) kinds will not interfere (assuming the C invariance of strong and electromagnetic interactions) unless the charges of the produced particles are distinguished, and (3) the contribution of the second diagram is found³ to be negligible if electrons are detected in the forward direction. We give a brief discussion of diagrams of Fig. 1(b) for $C = -$ states in Sec. VIII A.

To facilitate the calculation further we shall omit the Møller interference term in e^-e^- collisions. The effect of interference of electrons in the final states in e^-e^- collisions is clearly negligible since the amplitude for both incident electrons to scatter backwards is very small. In the case of e^-e^+ collisions we have already omitted the contribution of Bhabha-type terms, as was mentioned in the caption of Fig. 1.

Ideally speaking, it is of course desirable to detect scattered electrons in addition to produced particles. In the processes of our interest, however, most electrons are scattered into very small forward angles and are therefore hard to be separated from the unscattered beams by the present experimental technique. Furthermore, the counting rate becomes smaller as one specifies the final state more closely. For these reasons we shall discuss in this paper primarily those experiments in which electrons in the final state are not detected. Cross sections are relatively large in these cases and are therefore likely to be measured in the near future. In the case of e^+e^- colliding beams, however, this arrangement would make it difficult to distinguish between the e^+e^- annihilation process and the two-photon process. To avoid this problem it would be necessary to either measure the momenta of all produced particles accurately or detect at least one of the scattered electrons in coincidence with the produced particles. The latter approach may not be too unreasonable since, in order to distinguish these two processes, it suffices to detect the mere presence of the scattered electrons. Of course more quantitative information can be obtained (at the expense of diminishing cross

sections) if the energy and/or the angle of the scattered electron is measured. For the case where the energy (but not angle) of the scattered electron is measured, the cross sections can be easily derived from the cross sections in this and following sections by undoing the integration with respect to the energy of the scattered electron. Necessary modifications of the theory for the case in which electrons are detected scattering into

small forward angles are discussed briefly at the end of Sec. III. The case in which one of the electrons is scattered into large angles is treated in Sec. VIID and in a separate paper.¹⁷

We are now ready to write down the two-photon cross section for the process (1.1) for the production of $C=+$ state X integrated over the scattered-electron phase space (see Fig. 2 for the kinematics and notation):

$$d\sigma = \left(\frac{\alpha}{2\pi^2}\right)^2 \frac{1}{E^2} \int \frac{d^3p'_1}{E'_1} \int \frac{d^3p'_2}{E'_2} \left(\frac{1}{k_1^2 k_2^2}\right)^2 (2p_1^\mu p_1^\nu + \frac{1}{2} k_1^2 g^{\mu\nu}) (2p_2^\alpha p_2^\beta + \frac{1}{2} k_2^2 g^{\alpha\beta}) \times \frac{1}{8} M_{\mu\alpha}^\dagger M_{\nu\beta} d\bar{\Gamma},$$

$$M_{\mu\nu} = i \int d^4x e^{-ikx} \langle X | T^*(J_\mu(x) J_\nu(0)) | 0 \rangle, \quad (2.1)$$

$$d\bar{\Gamma} \equiv (2\pi)^4 \delta^4(k_1 + k_2 - p_X) d\Gamma,$$

where $d\Gamma = \prod_i [\rho_i d^3q_i (2\pi)^{-3}]$ is the invariant phase space of the state X [$\rho_i = 1/(2W_i)$ or m_i/W_i according as the particle i is a boson or a fermion], and p_X is the energy-momentum four-vector of the state X . The symbol T^* means that all Schwinger terms are subtracted in $M_{\mu\nu}$ so that both Lorentz covariance and gauge invariance are guaranteed. Throughout this paper we ignore, whenever it is safe, the electron mass m_e in comparison with the electron-beam energy E . In the following we shall refer to (2.1) as an exact formula (in contrast to the equivalent-photon-approximation formulas) even though some approximations have been made as explained above.

In the limit in which the photons of momenta k_1 and k_2 become real, the integrand of (2.1) satisfies the relation

$$\lim_{k_1^2 \rightarrow 0, k_2^2 \rightarrow 0} \frac{1}{8} M_{\mu\alpha}^\dagger M^{\mu\alpha} d\bar{\Gamma} = (2\omega_1)(2\omega_2) d\sigma_{\gamma\gamma \rightarrow X}, \quad (2.2)$$

where $d\sigma_{\gamma\gamma \rightarrow X}$ is the corresponding cross section for the production of the state X by two (oppositely directed) unpolarized photons of energy ω_1 and ω_2 , respectively. In the applications, we shall be interested in $d\sigma/ds$ where s is the invariant mass squared of the produced system:

$$s = (k_1 + k_2)^2 = m_X^2. \quad (2.3)$$

To exhibit the s dependence of the cross section, it is convenient to rewrite (2.1) by introducing the factor $\delta((k_1 + k_2)^2 - s)$ in its integrand and integrating the result over the variable s .

We shall introduce the variables ω , q , and \bar{s} by

$$\begin{aligned} \omega_1 &= E - E'_1 = \frac{1}{2}(\omega + q), \\ \omega_2 &= E - E'_2 = \frac{1}{2}(\omega - q), \\ \bar{s} &= \omega^2 - q^2 = 4\omega_1\omega_2. \end{aligned} \quad (2.4)$$

Then we can write (for $m_e^2 \ll E^2, E'^2$)

$$\delta((p_1 + p_2 - p'_1 - p'_2)^2 - s) = \delta(\bar{s} - 2(1 + \cos\theta')(E^2 + \frac{1}{4}\bar{s} - E\omega) - s), \quad (2.5)$$

where

$$\cos\theta' = \hat{p}'_1 \cdot \hat{p}'_2 = -\cos\theta'_1 \cos\theta'_2 + \sin\theta'_1 \sin\theta'_2 \cos\varphi'. \quad (2.6)$$

In the region where $\cos\theta'_i \sim 1$ ($i = 1, 2$) which gives the dominant contribution to the two-photon process, we have $\bar{s} \sim s$ and ω and q can be identified as the energy and momentum of the produced system X .

In terms of the new variables ω and \bar{s} , the \bar{s} integration can be carried out immediately and the required invariant lepton phase space becomes

$$\int \frac{d^3p'_1}{E'_1} \int \frac{d^3p'_2}{E'_2} \delta((p_1 + p_2 - p'_1 - p'_2)^2 - s) = \frac{1}{2} \pi \int_{-1}^1 dx_1 \int_{-1}^1 dx_2 \int_0^{2\pi} d\varphi' \int_{\sqrt{s}}^{E+s/4E} \frac{d\omega}{|q|} \sum_{q=\pm|q|} \frac{E'_1 E'_2 \theta(\omega^2 - \bar{s}_0)}{1 - \frac{1}{2}(1 + \cos\theta')}, \quad (2.7)$$

with

$$x_i = \cos \theta'_i, \quad i = 1, 2 \quad (2.8)$$

$$|q| = (\omega^2 - \bar{s}_0)^{1/2},$$

and

$$\bar{s}_0 = \frac{s + 2(1 + \cos \theta')(E^2 - E\omega)}{1 - \frac{1}{2}(1 + \cos \theta')} \quad (2.9)$$

The upper limit on ω is determined by the condition that E'_1 and E'_2 are positive. Notice also that \bar{s}_0 attains its minimum value $\bar{s}_{\min} = s$ for $\cos \theta' = -1$ or $\omega = E + s/4E$.

Aside from the omission of the Møller interference term and the approximation $m_e^2 \ll E^2, E'^2$, the cross section for the production of $C = +$ states by electron-electron collision is therefore given by¹⁸

$$\begin{aligned} \frac{d\sigma}{dsd\Gamma} = & \frac{\alpha^2}{8\pi^3} \int_{-1}^1 dx_1 \int_{-1}^1 dx_2 \int_0^{2\pi} d\varphi' \int_{\sqrt{s}}^{E+s/4E} \frac{d\omega}{|q|} \left(\frac{1}{k_1^2 k_2^2} \right)^2 (2\pi)^4 \delta^4(k_1 + k_2 - p_X) \frac{E'_1 E'_2}{E^2} \frac{\theta(\omega^2 - \bar{s}_0)}{1 - \frac{1}{2}(1 + \cos \theta')} \\ & \times (2p_1^\mu p_1^\nu + \frac{1}{2} k_1^2 g^{\mu\nu}) (2p_2^\alpha p_2^\beta + \frac{1}{2} k_2^2 g^{\alpha\beta}) \times \frac{1}{8} M_{\mu\alpha}^\dagger M_{\nu\beta} \end{aligned} \quad (2.10)$$

In practice, the four-dimensional integration can be handled in a straightforward manner by numerical integration.

III. APPLICATION OF THE EQUIVALENT-PHOTON METHOD TO THE TWO-PHOTON PROCESS

We shall now apply the equivalent-photon method described in the Appendix to the two-photon cross section $d\sigma$ [see (2.1)]. According to this method, the leading contribution to $d\sigma$ can be obtained by (1) performing the photon polarization sums in the radiation (Coulomb) gauge, (2) retaining only the transverse-current contribution, and (3) approximating the transverse current and the phase space $d\bar{\Gamma}$ by their values at $k_1^2 = k_2^2 = 0$, $\theta'_1 = \theta'_2 = 0$:

$$\begin{aligned} \sum_{i,j,l,m=1,2} (2p_1^i p_1^j - \frac{1}{2} k_1^2 g^{ij}) (2p_2^l p_2^m - \frac{1}{2} k_2^2 g^{lm}) \times \frac{1}{8} M_{il}^\dagger M_{jm} d\bar{\Gamma} \\ \Rightarrow \left(\frac{\vec{p}_1^2 \sin^2 \theta'_1}{k_1^2} - \frac{1}{2} k_1^2 \right) \left(\frac{\vec{p}_2^2 \sin^2 \theta'_2}{k_2^2} - \frac{1}{2} k_2^2 \right) (2\omega_1)(2\omega_2) d\sigma_{\gamma\gamma \rightarrow X}, \end{aligned} \quad (3.1)$$

where we have averaged over the azimuthal angles φ'_1, φ'_2 , and $d\sigma_{\gamma\gamma \rightarrow X}$ is defined by (2.2). Under these approximations the phase space $d\bar{\Gamma}$ loses all terms correlating the variables θ'_1, φ'_1 and θ'_2, φ'_2 . (Suppression of this correlation is an unavoidable feature in the simultaneous application of the equivalent-photon method to both electrons. It introduces an additional complication in this method whose effect is hard to evaluate.) The integrand of (2.1) also reduces to a product of two factors, one a function of θ'_1 and the other a function of θ'_2 . The integrations over the angles (θ'_1, φ'_1) and (θ'_2, φ'_2) of the scattered electrons can thus be carried out independently, giving

$$d\sigma^{(0)} = \int_0^E \frac{d\omega_1}{\omega_1} \int_0^E \frac{d\omega_2}{\omega_2} N(\omega_1) N(\omega_2) d\sigma_{\gamma\gamma \rightarrow X}(s), \quad (3.2)$$

as the leading approximation to the $C = +$ cross section, where $s = 4\omega_1\omega_2$ and $N(\omega)$ is given by (A7).

If we introduce the variables ω, q [see (2.4)], we obtain from (3.2) (putting $\bar{s} = s$)¹⁸

$$\begin{aligned} \frac{d\sigma^{(0)}}{dsd\Gamma} = & \frac{1}{s} \int_{\sqrt{s}}^{E+s/4E} \frac{d\omega}{|q|} N(\omega_1) N(\omega_2) \frac{d\sigma_{\gamma\gamma \rightarrow X}(s)}{d\Gamma} \\ = & 2 \left(\frac{\alpha}{\pi} \right)^2 \frac{1}{s} \frac{d\sigma_{\gamma\gamma \rightarrow X}(s)}{d\Gamma} \left[\left(\ln \frac{E}{m_e} - \frac{1}{2} \right)^2 f(\gamma) + \left(\ln \frac{E}{m_e} - \frac{1}{2} \right) g(\gamma) + h(\gamma) \right], \end{aligned} \quad (3.3)$$

where

$$\begin{aligned}
f(\gamma) &= \int_{\sqrt{s}}^{E+s/4E} \frac{d\omega}{|q|} \left(\frac{E^2+E_1'^2}{E^2} \right) \left(\frac{E^2+E_2'^2}{E^2} \right) \\
&= (2+\gamma^2)^2 \ln \frac{1}{\gamma} - (1-\gamma^2)(3+\gamma^2), \\
g(\gamma) &= \int_{\sqrt{s}}^{E+s/4E} \frac{d\omega}{|q|} \frac{E^2+E_1'^2}{E^2} N'(E_2') + \text{term with } 1 \leftrightarrow 2, \\
h(\gamma) &= \int_{\sqrt{s}}^{E+s/4E} \frac{d\omega}{|q|} N'(E_1')N'(E_2'),
\end{aligned} \tag{3.4}$$

and $\gamma = \sqrt{s}/2E$. Here $N'(E')$ is the last two terms in the square brackets of (A7) and vanishes for $E' \rightarrow E$.

The result (3.2) gives the relationship between the electron-electron collision and two-photon collision cross sections for the production of $C=+$ states in the equivalent-photon approximation. The remainder of the cross section [from the difference of (2.1) and (3.2)],¹⁸

$$\begin{aligned}
d\sigma^{(1)} &= \frac{\alpha^2}{8\pi^3} \int_{-1}^1 dx_1 \int_{-1}^1 dx_2 \int_0^{2\pi} d\varphi' \int_{\sqrt{s}}^{E+s/4E} \frac{d\omega}{|q|} \frac{E_1'E_2'}{E^2} \left(\frac{1}{k_1^2 k_2^2} \right)^2 \\
&\times \left[(2p_1^\mu p_1^\nu + \frac{1}{2} k_1^2 g^{\mu\nu}) (2p_2^\alpha p_2^\beta + \frac{1}{2} k_2^2 g^{\alpha\beta}) \times \frac{1}{8} M_{\mu\alpha}^\dagger M_{\nu\beta} d\tilde{\Gamma} \frac{\theta(\omega^2 - \bar{s}_0)}{1 - \frac{1}{2}(1 + \cos\theta')} \right. \\
&\left. - \left(\frac{\tilde{D}_1^{\alpha\beta} \tilde{D}_1^{\gamma\delta}}{k_1^2} \sin^2\theta'_1 - \frac{1}{2} k_1^2 \right) \left(\frac{\tilde{D}_2^{\alpha\beta} \tilde{D}_2^{\gamma\delta}}{k_2^2} \sin^2\theta'_2 - \frac{1}{2} k_2^2 \right) \left(\frac{1}{8} M_{\mu\alpha}^\dagger M^{\mu\alpha} d\tilde{\Gamma} \right)_{k_1^2=k_2^2=0, \theta'=\pi} \right], \tag{3.5}
\end{aligned}$$

can yield only a single power of $\ln(E/m_e)$ since the surviving contribution [from Coulomb excitation (scalar-longitudinal current contribution) and de-valuation of the transverse cross section from its value at $k_1^2 = k_2^2 = 0$, $\theta'_1 = \theta'_2 = 0$] is not singular when both k_1^2 and $k_2^2 \rightarrow 0$. Thus the equivalent-photon term $d\sigma^{(0)}$ dominates for large E/m_e provided there are no anomalous enhancements from the scalar current or variations of cross section with photon mass. The approximation

$$\sigma(E) \simeq 2 \left(\frac{\alpha}{\pi} \right)^2 \left(\ln \frac{E}{m_e} \right)^2 \int_{s_{\text{th}}}^{4E^2} \frac{ds}{s} \sigma_{\gamma\gamma \rightarrow X}(s) f \left(\frac{\sqrt{s}}{2E} \right) \tag{3.6}$$

is thus justified to order $[\ln(E/m_e)]^{-1}$, where s_{th} is the threshold value of s , and f is defined in (3.4).

We shall now discuss the angular spread of emitted (virtual) photons and scattered electrons. For this purpose we have to go back to the stage prior to (3.2) in which the integration over the angles θ'_1 and θ'_2 of the scattered electrons has not yet been carried out. It is easy to see that, for the small angular region, the differential cross section depends on the photon emission angle θ_γ or the electron scattering angle θ' as

$$\frac{d\theta_\gamma^2}{\theta_\gamma^2 + (m_e/E)^2}, \quad \frac{d\theta'^2}{\theta'^2 + [m_e(E-E')/EE']^2}, \tag{3.7}$$

respectively. [Although the second formula seems to lead to a $\ln(E-E')$ singularity, it is actually suppressed in the complete expression. See Eq. (A7).] Thus, roughly $\frac{1}{2}$ of the cross section comes

from the angles

$$\theta_\gamma, \theta' < (m_e/E)^{1/2}, \tag{3.8}$$

and roughly $\frac{3}{4}$ comes from $\theta_\gamma, \theta' < (m_e/E)^{1/4}$, etc. This spreading of the virtual photon beam is expected to introduce errors of order $(m_e/E)^{1/2}$ in the angular distribution of produced particles. In this region we can usually neglect hadronic form-factor effects. Thus the dominant contribution to the process $e+e \rightarrow e+e+X$ can be represented as photon-photon collisions of two oppositely directed bremsstrahlung beams each of virtual radiator strength $N \sim (2\alpha/\pi) \ln(E/m_e)$ and beam angular divergence $\sim (m_e/E)^{1/2}$.

It is easy to extend our considerations to the case in which either or both electrons are detected scattering into the small forward angles

$$\theta'_1, \theta'_2 < \theta_{\text{max}}, \quad (m_e/E)^2 \ll \theta_{\text{max}}^2 \ll 1. \tag{3.9}$$

In the equivalent-photon approximation, the corresponding cross section is given by the formula (3.2) if we replace $N(\omega)$ by

$$\begin{aligned}
N(\omega, \theta_{\text{max}}) &= \frac{\alpha}{\pi} \left[\frac{E^2+E'^2}{E^2} \left(\ln \frac{E\theta_{\text{max}}}{2m_e} - \frac{1}{2} \right) \right. \\
&\quad \left. + \frac{(E-E')^2}{2E^2} \left(\ln \frac{2E'}{E-E'} + 1 \right) \right. \\
&\quad \left. + \frac{(E+E')^2}{2E^2} \ln \frac{2E'}{[(E-E')^2 + EE'\theta_{\text{max}}^2]^{1/2}} \right], \tag{3.10}
\end{aligned}$$

which is obtained by restricting the domain of in-

tegration to $0 \leq \theta' \leq \theta_{\max}$ in (A7). In the case $\theta_{\min} \leq \theta' \leq \theta_{\max}$ $[(m_e/E)^2 \ll \theta_{\min}^2]$, $N(\omega)$ should be replaced by $N(\omega, \theta_{\max}) - N(\omega, \theta_{\min})$. Note that the correction term $d\sigma^{(1)}$ given by (3.5) vanishes as $O(\theta_{\max}^2)$. Thus, the equivalent-photon result approaches the exact cross section in the case where both scattered electrons are detected within small forward angles. Of course we have assumed here that the scalar-longitudinal current contribution is not abnormally large: $\theta_{\max}^2 |M_{\text{long}}|^2 \ll |M_{\text{trans}}|^2$.

IV. TEST OF VALIDITY OF EQUIVALENT-PHOTON APPROXIMATION IN NARROW-RESONANCE PRODUCTION

The simplest example of hadron production by electron-electron collision is the narrow-resonance meson production (π^0 , η , η' , etc.). We shall first consider the case of π^0 production in some detail in order to see how well the equivalent-photon approximations are justified in practice. We take the effective Lagrangian for the $\pi^0 - 2\gamma$ coupling

$$\mathcal{L}_I = (g/2!) \epsilon^{\mu\nu\kappa\lambda} F_{\mu\nu} F_{\kappa\lambda} \varphi_\pi. \quad (4.1)$$

This gives

$$g^2 = 4\pi\Gamma_{\pi^0 \rightarrow 2\gamma} / m_\pi^3, \quad (4.2)$$

where m_π is the mass of the π^0 , $\Gamma_{\pi^0 \rightarrow 2\gamma} = \tau_{\pi^0}^{-1}$ is the $\pi^0 \rightarrow 2\gamma$ decay width, and

$$\sigma_{\gamma\gamma \rightarrow \pi^0} = \frac{8\pi^2\Gamma_{\pi^0 \rightarrow 2\gamma}}{m_\pi} \delta(m_\pi^2 - s) \quad (4.3)$$

is the narrow-width production cross section of π^0 at $k_1^2 = k_2^2 = 0$. [In the case of spin- J production there is an additional factor of $2J+1$ in (4.3).] Thus the leading term of the total cross section for $e+e \rightarrow e+e+\pi^0$ in the equivalent-photon approximation is^{12, 19}

$$\sigma_{ee \rightarrow ee\pi^0}^{(0)} = \frac{16\alpha^2\Gamma_{\pi^0 \rightarrow 2\gamma}}{m_\pi^3} \times \left[\left(\ln \frac{E}{m_e} - \frac{1}{2} \right)^2 f(\gamma) + \left(\ln \frac{E}{m_e} - \frac{1}{2} \right) g(\gamma) + h(\gamma) \right] \quad (4.4)$$

from (3.3) where $\gamma = m_\pi/2E$. The $g(\gamma)$ and $h(\gamma)$ terms contribute only 0.5% at $E=2$ GeV and can be neglected. The result using $\Gamma_{\pi^0 \rightarrow 2\gamma} = 8.6$ eV is plotted in Fig. 3. See also Table I. It should be noted that the present experimental error in $\Gamma_{\pi^0 \rightarrow 2\gamma}$ is ± 1.7 eV.²⁰

This equivalent-photon-approximation result can be compared with the exact fourth-order calculation. The quantity

$$(2p_1^\mu p_1^\nu + \frac{1}{2} k_1^2 g^{\mu\nu}) (2p_2^\alpha p_2^\beta + \frac{1}{2} k_2^2 g^{\alpha\beta}) \times \frac{1}{8} M_{\mu\alpha}^\dagger M_{\nu\beta} d\bar{\Gamma}$$

in the integrand of (2.1) can be written in this case

as

$$2g^2 B |F|^2 \times 2\pi\delta((k_1+k_2)^2 - m_\pi^2), \quad (4.5)$$

where

$$\begin{aligned} B &= \frac{1}{4} k_1^2 k_2^2 B_1 - 4B_2^2 + m_e^2 B_3, \\ B_1 &= (4p_1 \cdot p_2 - 2p_1 \cdot k_2 - 2p_2 \cdot k_1 + k_1 \cdot k_2)^2 \\ &\quad + (k_1 \cdot k_2)^2 - k_1^2 k_2^2 - 16m_e^4, \\ B_2 &= (p_1 \cdot p_2)(k_1 \cdot k_2) - (p_1 \cdot k_2)(p_2 \cdot k_1), \\ B_3 &= k_1^2 (2p_1 \cdot k_2 - k_1 \cdot k_2)^2 \\ &\quad + k_2^2 (2p_2 \cdot k_1 - k_1 \cdot k_2)^2 + 4m_e^2 (k_1 \cdot k_2)^2. \end{aligned} \quad (4.6)$$

The factor F is included in (4.5) to represent possible form-factor dependency of the cross section on the photon masses:

$$F = F(k_1^2, k_2^2) \text{ with } F(0, 0) = 1. \quad (4.7)$$

In Fig. 3 (see also Table I) we have plotted the result for $\sigma_{ee \rightarrow ee\pi^0}$ obtained by numerical integration of (2.10) and (4.5) assuming the cases

$$(a) F = 1 \quad (4.8)$$

and

$$(b) F = (1 - k_1^2/m_\rho^2)^{-1} (1 - k_2^2/m_\rho^2)^{-1}, \quad (4.9)$$

as suggested by ρ dominance. It is seen that the

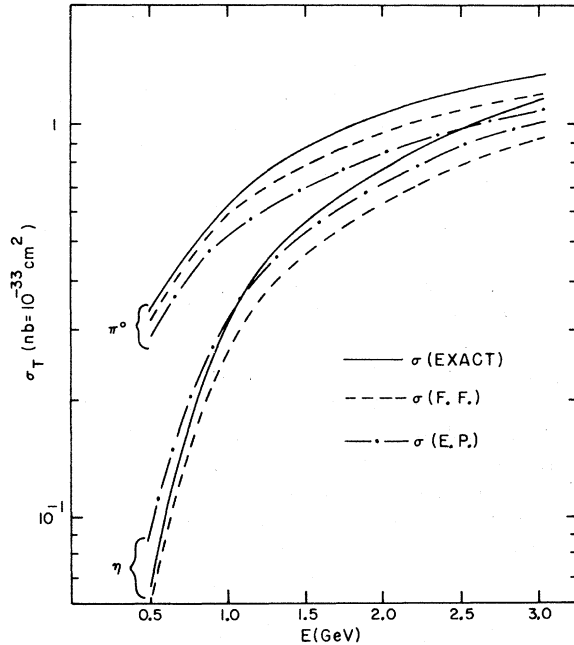


FIG. 3. The total cross sections for the colliding-beam production of π^0 and η . Exact, f.f., and e.p. refer to the cross sections calculated without form factors, with the form factor (4.9) suggested by ρ dominance, and in the equivalent-photon approximation, respectively.

TABLE I. The total cross sections for the colliding-beam production of π^0 , η , $\mu^+\mu^-$, e^+e^- , $\pi^+\pi^-$. Exact, f.f., and e.p. refer to the cross sections calculated without form factor, with form factor (4.9), and in the equivalent-photon approximation, respectively.

Process	E (GeV)					
	0.5	1.0	1.5	2.0	2.5	3.0
	$\sigma_{\text{total}}(10^{-33} \text{ cm}^2)$					
$ee \rightarrow ee\pi^0$ (exact)	0.33	0.63	0.88	1.06	1.24	1.38
$ee \rightarrow ee\pi^0$ (f.f.)	0.31	0.59	0.78	0.95	1.10	1.18
$ee \rightarrow ee\pi^0$ (e.p.)	0.28	0.53	0.69	0.85	0.96	1.07
$ee \rightarrow ee\eta$ (exact)	0.067	0.32	0.56	0.77	0.98	1.16
$ee \rightarrow ee\eta$ (f.f.)	0.062	0.27	0.46	0.63	0.79	0.92
$ee \rightarrow ee\eta$ (e.p.)	0.086	0.32	0.54	0.70	0.89	1.00
$ee \rightarrow ee\mu^+\mu^-$ (e.p.)	8.1	18.7	29	38	45	50
$ee \rightarrow ee\pi^+\pi^-$ (e.p.)	0.46	1.37	2.2	2.9	3.5	4.1
$ee \rightarrow eee^+e^-$ (e.p.)	5.5×10^6	7.3×10^6	8.4×10^6	9.5×10^6	1.02×10^7	1.09×10^7
$e^+e^- \rightarrow \mu^+\mu^-$	87	22	9.7	5.4	3.5	2.4
$e^+e^- \rightarrow \pi^+\pi^-$ (pointlike)	22	5.4	2.4	1.36	0.87	0.60

equivalent-photon approximation underestimates the total cross section by 20–30% for $1 \leq E \leq 3$ GeV. However, the exact result is reduced considerably when the effect of the form factor (4.9) is taken

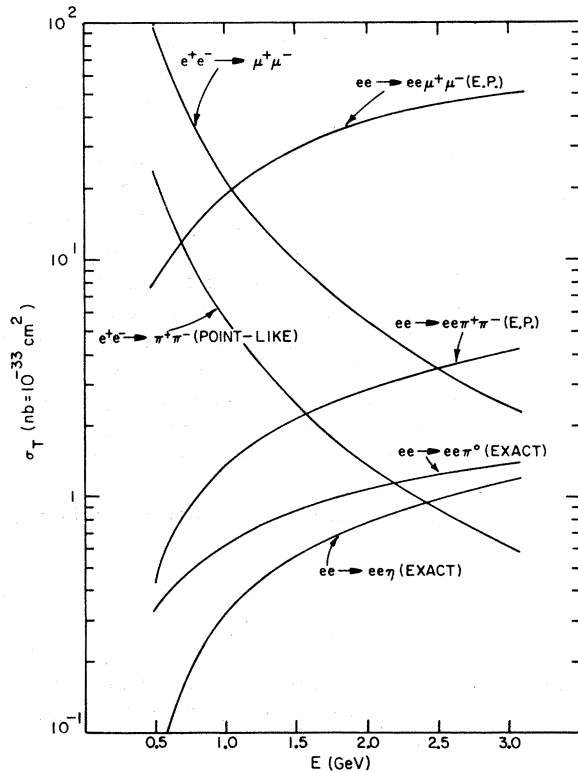


FIG. 4. The total cross sections for the colliding-beam production of π^0 , η , $\pi^+\pi^-$, and $\mu^+\mu^-$. The cross sections for π^0 and η are exact and without form factors. The two-photon cross sections for $\pi^+\pi^-$ and $\mu^+\mu^-$ are calculated in the equivalent-photon approximation. See Ref. 7 for the discrepancy between this figure and Fig. 2 of Ref. 2.

into account.

The discrepancy between the equivalent-photon and exact calculations can be traced to the contribution to the total cross section of relatively large electron scattering angles.²¹ Note that for $\theta_\gamma > (m_e/E)^{1/4}$ ($\sim 12^\circ$ for $E=1$ GeV), which still contains approximately 25% of the total cross section (see Sec. III), $|k_1^2|$ is larger than m_π^2 . The equivalent-photon approximation is not expected to work well in this region since, roughly speaking, it can be regarded as an expansion in k_1^2/m_π^2 . For the same reason this approximation is more reliable for the production of more massive states such as η and η' . The exact (with and without form factors) and approximate total cross sections for η production are shown in Fig. 3. See also Table I. We have used $m_\eta = 0.549$ GeV and $\Gamma_{\eta \rightarrow 2\gamma} = 1.0$ keV.²⁰

Thus, as far as present predictions of $C=+$ hadron production by electron-electron collisions are concerned, the equivalent-photon approximation is adequate since errors due to lack of knowledge of coupling constants, form factors, etc., are much more serious. The detailed fitting of the decay width and the possible determination of form factors and longitudinal current contributions (from large-angle electron scattering) to resonance production will require, however, the complete result.

Further examples of narrow-resonance production are discussed in Sec. IX.

V. TWO-PHOTON CROSS SECTIONS FOR $\pi^+\pi^-$ AND $\mu^+\mu^-$ PRODUCTION IN THE EQUIVALENT-PHOTON APPROXIMATION

In this section we shall discuss the two-photon production of a $\pi^+\pi^-$ (or $\mu^+\mu^-$) pair

$$e^+e^- \rightarrow e^+e^+\pi^+\pi^-, \quad (5.1)$$

$$e+e \rightarrow e+e+\mu^+\mu^-, \quad (5.2)$$

by colliding electron beams. The analysis of π^0 production described in Sec. IV shows that the important features of the $\pi^+\pi^-$ (or $\mu^+\mu^-$) production cross section, except for the coplanarity of pion

(muon) pairs to be discussed in Sec. VII, can be investigated with reasonable accuracy by means of the equivalent-photon method. We shall therefore restrict ourselves here to this approximation, leaving the exact calculation to a later section.

A. Total Cross Sections

Calculation of the two-photon total cross section for muon pair production is straightforward in the equivalent-photon approximation. We simply have to substitute the total cross section for the $\mu^+\mu^-$ pair creation by two γ 's,²²

$$\sigma_{\gamma\gamma \rightarrow \mu^+\mu^-}(s) = \frac{4\pi\alpha^2}{s} \left\{ \left(2 + \frac{8m_\mu^2}{s} - \frac{16m_\mu^4}{s^2} \right) \ln \left[\frac{\sqrt{s}}{2m_\mu} + \left(\frac{s}{4m_\mu^2} - 1 \right)^{1/2} \right] - \left(1 - \frac{4m_\mu^2}{s} \right)^{1/2} \left(1 + \frac{4m_\mu^2}{s} \right) \right\}, \quad (5.3)$$

into the formula (3.6). The result of numerical calculation is plotted in Fig. 4 (see also Table I). This cross section exceeds the one-photon cross section $\sigma_{e^+e^- \rightarrow \mu^+\mu^-}$, which is equal to

$$\frac{\pi\alpha^2}{3E^2} \left(1 - \frac{m_\mu^2}{E^2} \right)^{1/2} \left(1 + \frac{m_\mu^2}{2E^2} \right),$$

for $E \geq 1$ GeV. For very large E/m_e we have²³

$$\sigma_{ee \rightarrow ee\mu^+\mu^-}(E) \simeq \frac{112\alpha^4}{9\pi} \frac{1}{m_\mu^2} \left(\ln \frac{E}{m_e} \right)^2 \ln \frac{E}{m_\mu}. \quad (5.4)$$

Note also that in the energy range shown in Fig. 4, the $\mu^+\mu^-$ -production cross section (both one-photon and two-photon processes) is an order of magnitude larger than any process of hadron production. Since the muon is pointlike as far as it has been tested experimentally, this cross section is undoubtedly the most reliably known of cross sections shown in Fig. 4.

The evaluation of the total cross section for pion-pair production is not as simple as the muon case because of the strong interaction in the final state. In fact, the reaction (5.1) is the ideal process for studying the $\pi\pi$ interaction in $C=+$ states such as the σ and ϵ resonances. However, we shall postpone the consideration of hadron physics until Sec. VI and, for illustration, first treat π^+ and π^- as pointlike charged particles without strong interaction. There are two reasons for doing this: (1) Such a calculation serves as the reference point of hadron physics because the effect of strong interaction in the final state can be determined as the deviation of the cross section from the one calculated here. (2) For E around 1 GeV, our calculation will in fact give a reasonable estimate of the actual cross section for $\pi^+\pi^-$ production. This is because the small- s region near the threshold is not too far removed from the threshold region of the elastic photon-pion scattering, where the exact value of the cross section is determined by the low-energy theorem for Compton scattering, and because the contribution of $\sigma_{\gamma\gamma \rightarrow \pi^+\pi^-}(s)$ to the integral (3.6) is heavily weighted towards the low- s end.

If we accept this picture as the first approximation, $\sigma_{\gamma\gamma \rightarrow \pi^+\pi^-}$ can be calculated from the Born (including seagull) diagrams and is given by²⁴

$$\sigma_{\gamma\gamma \rightarrow \pi^+\pi^-}(s) = \frac{2\pi\alpha^2}{s} \left\{ \left(1 + \frac{4m_\pi^2}{s} \right) \left(1 - \frac{4m_\pi^2}{s} \right)^{1/2} - \frac{8m_\pi^2}{s} \left(1 - \frac{2m_\pi^2}{s} \right) \ln \left[\frac{\sqrt{s}}{2m_\pi} + \left(\frac{s}{4m_\pi^2} - 1 \right)^{1/2} \right] \right\}. \quad (5.5)$$

In Fig. 4 (see also Table I) we show the energy dependence of the total cross section for the colliding-beam production of the $\pi^+\pi^-$ pair calculated from (5.5) in the equivalent-photon approximation. This cross section exceeds the usual one-photon cross section $\sigma_{e^+e^- \rightarrow \pi^+\pi^-}$, which equals

$$\frac{\pi\alpha^2}{12E^2} \left(1 - \frac{m_\pi^2}{E^2} \right)^{3/2}$$

for pointlike pions for $E > 1.5$ GeV.⁷ For very large E/m_e , we have²⁵

$$\sigma_{ee \rightarrow ee\pi^+\pi^-}(E) \simeq \frac{16\alpha^4}{9\pi} \frac{1}{m_\pi^2} \left(\ln \frac{E}{m_e} \right)^2 \ln \frac{E}{m_\pi}. \quad (5.6)$$

B. Angular Distributions

We shall now discuss the angular distribution of the produced pair. For this purpose we need the differential cross sections for $\gamma + \gamma \rightarrow \mu^+ + \mu^-$ (Ref. 26) and $\gamma + \gamma \rightarrow \pi^+ + \pi^-$ (Ref. 27):

$$\frac{d\sigma_{\gamma\gamma \rightarrow \mu^+\mu^-}}{d\Omega_1} = \frac{\alpha^2}{2s} \left(1 - \frac{4m_\mu^2}{s}\right)^{1/2} G_\mu(W_1, \theta_1), \quad (5.7)$$

$$G_\mu(W_1, \theta_1) = 2 + 4 \left(1 - \frac{m_\mu^2}{W_1^2}\right) \frac{(1 - m_\mu^2/W_1^2)\sin^2\theta_1 \cos^2\theta_1 + m_\mu^2/W_1^2}{[1 - (1 - m_\mu^2/W_1^2)\cos^2\theta_1]^2} + \frac{s/W_1^2 - 4}{1 - (1 - m_\mu^2/W_1^2)\cos^2\theta_1},$$

and

$$\frac{d\sigma_{\gamma\gamma \rightarrow \pi^+\pi^-}}{d\Omega_1} = \frac{\alpha^2}{2s} \left(1 - \frac{4m_\pi^2}{s}\right)^{1/2} G_\pi(W_1, \theta_1), \quad (5.8)$$

$$G_\pi(W_1, \theta_1) = 1 - \frac{2m_\pi^2}{W_1^2} \left(1 - \frac{m_\pi^2}{W_1^2}\right) \frac{\sin^2\theta_1}{[1 - (1 - m_\pi^2/W_1^2)\cos^2\theta_1]^2},$$

where W_1 is the energy of μ^+ (or π^+), and θ_1 is the angle between one of the incident photons and an outgoing μ^+ (or π^+) in the photon-photon center-of-mass system. Before we substitute these cross sections into (3.3), we have to transform them from the photon-photon center-of-mass system to the electron-electron center-of-mass system. For this purpose it is useful to note that $G_\mu(W_1, \theta_1)$ and $G_\pi(W_1, \theta_1)$ are form-invariant under the Lorentz transformation along the beam direction. Thus we have only to reinterpret W_1 and θ_1 in $G_\mu(W_1, \theta_1)$ and $G_\pi(W_1, \theta_1)$ as the energy and angle of μ^+ (or π^+) in the laboratory frame (i.e., the electron-electron center-of-mass system). In this way we can derive various differential cross sections from (3.3). Of particular interest are [the superscript (0) refers to the equivalent-photon approximation as in (3.2)]

$$\frac{d\sigma_{ee \rightarrow ee\pi^+\pi^-}^{(0)}}{d\Omega_1} = \frac{8\alpha^4}{\pi^2} \left(\ln \frac{E}{m_e}\right)^2 \int_{4m_\pi^2}^{4E^2} \frac{ds}{s^2} \int_{-q_m}^{q_m} \frac{dq}{\omega} G_\pi(W_1, \theta_1) \frac{(E^2 + E_1'^2)(E^2 + E_2'^2)}{4E^4} \frac{|\vec{q}_1|^2}{[s^2 - 4m_\pi^2(\omega^2 - q^2 \cos^2\theta_1)]^{1/2}}, \quad (5.9)$$

with

$$q_m = E - s/4E, \quad \omega = (q^2 + s)^{1/2},$$

$$|\vec{q}_1| = \frac{sq \cos\theta_1 + \omega[s^2 - 4m_\pi^2(\omega^2 - q^2 \cos^2\theta_1)]^{1/2}}{2(\omega^2 - q^2 \cos^2\theta_1)}, \quad W_1 = (|\vec{q}_1|^2 + m_\pi^2)^{1/2}, \quad (5.10)$$

and

$$\frac{d\sigma_{ee \rightarrow ee\pi^+\pi^-}^{(0)}}{d\Omega_1 d\Omega_2} = \frac{4\alpha^4}{\pi^2} \left(\ln \frac{E}{m_e}\right)^2 \int_{4m_\pi^2}^{4E^2} \frac{ds}{s^2} G_\pi(W_1, \theta_1) \frac{(E^2 + E_1'^2)(E^2 + E_2'^2)}{4E^4} \frac{|\vec{q}_1|^2 |\vec{q}_2| \sin(\theta_2 - \theta_1)}{q[\omega W_1 \sin^2\theta_1 + \omega W_2 \sin^2\theta_2 - W_1 W_2 \sin^2(\theta_2 - \theta_1)]} \quad (5.11)$$

for $\theta_1 < \theta_2$ with

$$a_1 = [\sin\theta_1/\sin(\theta_2 - \theta_1)]^2, \quad a_2 = [\sin\theta_2/\sin(\theta_2 - \theta_1)]^2,$$

$$q^2 = \frac{2[a_1 a_2 s^2 - m_\pi^2(a_1 + a_2 - (a_1 - a_2)^2)s + m_\pi^4]^{1/2} - (a_1 + a_2 - 1)s - 2m_\pi^2}{4a_1 a_2 - (a_1 + a_2 - 1)^2},$$

$$|\vec{q}_1| = q \sin\theta_2/\sin(\theta_2 - \theta_1), \quad |\vec{q}_2| = q \sin\theta_1/\sin(\theta_2 - \theta_1), \quad (5.12)$$

$$W_2 = (|\vec{q}_2|^2 + m_\pi^2)^{1/2}, \quad q^2 \leq q_m^2.$$

θ_1 and θ_2 are the angles of π^+ and π^- with respect to the electron beam direction. Other notations are defined in Fig. 2. We can use the symmetry property $d\sigma(\pi - \theta_1, \pi - \theta_2) = d\sigma(\theta_1, \theta_2)$ in order to obtain the cross section for $\theta_1 > \theta_2$ from (5.11). Cross sections for muon pair production (5.2) are obtained by replacing $G_\pi(W_1, \theta_1)$ with $G_\mu(W_1, \theta_1)$ in (5.9) and (5.11).

In Fig. 5 (see also Table II) we show the cross section $d\sigma_{ee \rightarrow ee\pi^+\pi^-}^{(0)}/d\Omega_1$ calculated from (5.9) for $E = 1, 2,$ and 3 GeV. It is clearly seen that the pions are produced predominantly in the beam direction. For comparison, the one-photon cross section $d\sigma_{ee \rightarrow ee\pi^+\pi^-}^{\text{pointlike}}/d\Omega_1$ is also shown for $E = 1$ GeV.

In Figs. 6-14 (see also Table III) we show the cross section $d\sigma_{ee \rightarrow ee\pi^+\pi^-}^{(0)}/d\Omega_1 d\Omega_2$ calculated from (5.11) for combinations of $\theta_1 = 5.7^\circ, 30^\circ,$ and 90° and $E = 1, 2,$ and 3 GeV. One can observe a strong tendency that the

pion pairs are likely to be produced with a rather narrow opening angle. That is, the pion pairs tend to come out in a strongly noncollinear fashion. This is in contrast to the pion pairs produced in the one-photon process, which must be exactly collinear.

For comparison we also show in Fig. 15 $d\sigma_{ee \rightarrow ee\mu^+\mu^-}^{(0)}/d\Omega_1$, and $d\sigma_{ee \rightarrow ee\mu^+\mu^-}^{(0)}/d\Omega_1 d\theta_2$ in Figs. 16–18 for $E=1$ GeV which show even stronger peaking in the beam direction than the pion case. For details see also Tables IV and V.²⁸

C. Bias Factor

The figures for the various cross sections shown above are somewhat misleading because they do not take explicit account of the diminishing phase space as the pions approach the beam direction. In order to evaluate this effect and also to exhibit some of the features of these cross sections more clearly, let us examine the cross section

$$\begin{aligned} \frac{d\sigma_{ee \rightarrow ee\pi^+\pi^-}^{(0)}}{dsd\Omega} &= \left(\frac{2\alpha}{\pi}\right)^2 \left(\ln \frac{E}{m_e}\right)^2 \int_{-a_m}^{a_m} \frac{dq}{\omega} \theta(s^2 - 4m_\pi^2(\omega^2 - q^2 \cos^2 \theta)) \\ &\times \frac{(E^2 + E_1'^2)(E^2 + E_2'^2)}{4E^4} \frac{1}{(1 - 4m_\pi^2/s)^{1/2}} \frac{d\sigma_{\gamma\gamma \rightarrow \pi^+\pi^-}}{d\Omega} \frac{\{sq \cos \theta + \omega[s^2 - 4m_\pi^2(\omega^2 - q^2 \cos^2 \theta)]^{1/2}\}^2}{s(\omega^2 - q^2 \cos^2 \theta)^2 [s^2 - 4m_\pi^2(\omega^2 - q^2 \cos^2 \theta)]^{1/2}}. \end{aligned} \quad (5.13)$$

This expression becomes considerably simpler in the region

$$\omega^2 \ll E^2, \quad (5.14)$$

where we can simplify the virtual-photon distribution, and

$$\tilde{q}_i^2 \gg m_\pi^2, \quad i=1, 2 \quad (5.15)$$

where we can ignore the complications from the pion's velocity. Then $d\sigma_{\gamma\gamma \rightarrow \pi^+\pi^-}/d\Omega$ becomes isotropic in the photon-photon center-of-mass system and hence u -independent for fixed s , where $u=q/\omega$ is the velocity of the photon-photon center-of-mass system as seen in the laboratory frame. Thus Eq. (5.13) reduces to

$$\begin{aligned} \frac{d\sigma_{ee \rightarrow ee\pi^+\pi^-}^{(0)}}{dsd\Omega} &= \left(\frac{2\alpha}{\pi}\right)^2 \left(\ln \frac{E}{m_e}\right)^2 \frac{1}{s} \int_{-u_m}^{u_m} \frac{du}{(1 - u \cos \theta)^2} \frac{d\sigma}{d\Omega} \\ &= \left(\frac{2\alpha}{\pi}\right)^2 \left(\ln \frac{E}{m_e}\right)^2 \frac{2}{s} \frac{u_m}{1 - u_m^2 \cos^2 \theta} \frac{d\sigma}{d\Omega}, \quad 4m_\pi^2 \ll s \ll 4E^2, \end{aligned} \quad (5.16)$$

where $u_m = (1 - s/4E^2)/(1 + s/4E^2)$ is the maximum velocity allowed kinematically. It is seen from (5.16) that the angular distribution is peaked along the beam direction, with the peaking becoming more pronounced as the mass \sqrt{s} of the system decreases.

In order to understand how this peaking affects experiments which are usually only sensitive to particles produced at large angles, we can define a bias factor

$$G_{\Delta\Omega}(s) = \int_{\Delta\Omega} \frac{d\sigma_{ee \rightarrow eeX}}{dsd\Omega} \frac{d\Omega}{ds} \frac{\Delta\Omega}{4\pi}, \quad (5.17)$$

which gives the ratio of the efficiency of detecting events in a given solid angle $\Delta\Omega$ compared to the efficiency of detecting events in $\Delta\Omega$ if the events were isotropic in the laboratory. For the usual experimental arrangement with symmetry in the φ coordinate, and for

$$-x_0 < \cos \theta < x_0, \quad 0 < x_0 \leq 1 \quad (5.18)$$

the efficiency ratio for the cross section (5.16) will be

$$\begin{aligned} G_{\Delta\Omega}(s) &= \int_{-x_0}^{x_0} \frac{dx}{1 - u_m^2 x^2} / x_0 \int_{-1}^1 \frac{dx}{1 - u_m^2 x^2} \\ &= \frac{1}{x_0} \frac{\ln[(1 + u_m x_0)/(1 - u_m x_0)]}{\ln[(1 + u_m)/(1 - u_m)]}. \end{aligned} \quad (5.19)$$

We note that for s large ($u_m \ll 1$)

$$G_{\Delta\Omega}(s) \simeq 1 - \frac{1}{3} u_m^2 (1 - x_0^2), \quad (5.20)$$

which is a negligible bias. For $s/4E^2 \ll 1$, $u_m \simeq 1 - 2(s/4E^2)$ and we have

$$G_{\Delta\Omega}(s) \simeq \frac{\ln[(1 + x_0)/(1 - x_0)]}{x_0 \ln(4E^2/s)}. \quad (5.21)$$

For example,

$$G_{\Delta\Omega}(s) \simeq 0.53 \quad \text{for } x_0 = (\frac{1}{2})^{1/2}, \quad s/4E^2 = \frac{1}{100}. \quad (5.22)$$

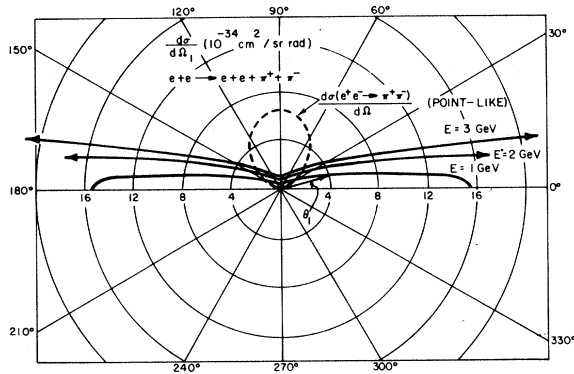


FIG. 5. The cross section $d\sigma/d\Omega_1$ for the process $e+e \rightarrow e+e+\pi^++\pi^-$ calculated in the equivalent-photon approximation for $E=1, 2,$ and 3 GeV. For comparison, the one-photon cross section $d\sigma_{e^+e^- \rightarrow \pi^+\pi^-}^{\text{pointlike}}/d\Omega_1$ is also shown for $E=1$ GeV. See Table II for further information.

Thus, if $d\sigma_{\gamma\gamma \rightarrow \pi^+\pi^-}$ were isotropic in the photon-photon center-of-mass system, the bias factor is only a logarithmic effect and does not give worse than 50% loss in counting rate. Actually, the non-isotropic part of the cross section for $\pi^+\pi^-$ production will be relatively small, as is seen from (5.8), and the above estimate will not be affected too much. For the production of the $\mu^+\mu^-$ pair, however, the cross section is strongly nonisotropic and the bias factor would be much smaller than the above estimate. In both the $\pi^+\pi^-$ and the $\mu^+\mu^-$ cases, the exact value of the bias factor can be obtained easily by numerical integration.

VI. STRONG-INTERACTION MODIFICATIONS

OF $\gamma+\gamma \rightarrow \pi^++\pi^-$

A. General Features

One of the most basic processes which can be studied by electron-electron collisions is $\gamma+\gamma \rightarrow \pi^++\pi^-$. In general, the full Compton amplitude for k_1^2, k_2^2 spacelike and

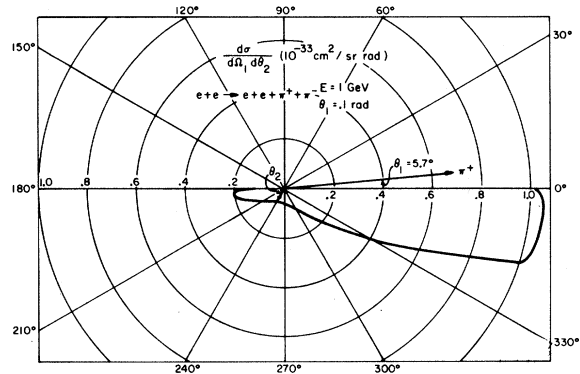


FIG. 6. The cross section $d\sigma/d\Omega_1d\theta_2$ for the process $e+e \rightarrow e+e+\pi^++\pi^-$ calculated in the equivalent-photon approximation. $E=1$ GeV, $\theta_1=5.7^\circ$.

$$s = (k_1 + k_2)^2 = (q_1 + q_2)^2 > 4m_\pi^2$$

can be studied. However, until very-high-luminosity rings are constructed, we will have to content ourselves with the case of (almost) real photons.

In the Born approximation (no strong interactions) the amplitude for $\gamma+\gamma \rightarrow \pi^+\pi^-$ is $e^2\epsilon_\mu(k_1)M_B^{\mu\nu}\epsilon_\nu(k_2)$, where

$$M_B^{\mu\nu} = -2g^{\mu\nu} + \frac{(2q_1^\mu - k_1^\mu)(2q_2^\nu - k_2^\nu)}{2q_1 \cdot k_1} + \frac{(2q_1^\nu - k_2^\nu)(2q_2^\mu - k_1^\mu)}{2q_2 \cdot k_1}. \quad (6.1)$$

In the general case, gauge invariance, parity conservation, and time-reversal invariance limit the complete structure to two independent amplitudes. A convenient parametrization is

$$M^{\mu\nu} = M_B^{\mu\nu} B(s, t, u) + 4(g^{\mu\nu} k_1 \cdot k_2 - k_1^\nu k_2^\mu) A(s, t, u). \quad (6.2)$$

This form has only the explicit poles dictated by the Born contribution. The Thomson limit for

TABLE II. The cross section $d\sigma/d\Omega_1$ for the process $e+e \rightarrow e+e+\pi^++\pi^-$ calculated in the equivalent-photon approximation for $E=1, 2,$ and 3 GeV. The one-photon cross section $d\sigma_{e^+e^- \rightarrow \pi^+\pi^-}^{\text{pointlike}}/d\Omega_1$ is also given for $E=1$ GeV.

E (GeV)	θ_1 (deg)							
	1.0	5.7	11.5	17.2	22.9	30	60	90
$d\sigma_{ee \rightarrow ee\pi^+\pi^-}/d\Omega_1$ (10^{-34} cm ² /sr)								
1.0	15.2	10.3	5.6	3.6	2.3	1.62	0.58	0.44
2.0	85	37	13.6	7.6	4.6	3.1	1.02	0.75
3.0	191	49	21	10.6	6.4	4.2	1.28	0.93
$d\sigma_{e^+e^- \rightarrow \pi^+\pi^-}^{\text{pointlike}}/d\Omega_1$ (10^{-34} cm ² /sr)								
1.0	2.0×10^{-3}	0.065	0.26	0.57	0.99	1.62	4.9	6.5

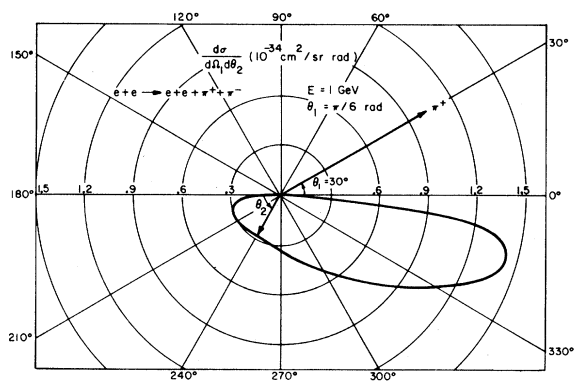


FIG. 7. The cross section $d\sigma/d\Omega_1 d\theta_2$ for the process $e+e \rightarrow e+e+\pi^++\pi^-$ calculated in the equivalent-photon approximation. $E=1$ GeV, $\theta_1=30^\circ$.

forward Compton scattering, of course, demands $B(0, m_\pi^2, m_\pi^2)=1$. In addition to the usual conditions from crossing (A and B are even under $t \rightarrow u$), unitarity to order e^2 requires

$$\text{Im } F_{\gamma\gamma \rightarrow \pi\pi}^J \propto F_{\gamma\gamma \rightarrow \pi\pi}^{J*} F_{\pi\pi \rightarrow \pi\pi}^J. \quad (6.3)$$

This relation holds for each amplitude of given angular momentum J (in the photon-photon center-of-mass system) and isotopic spin if s is in the region of $\pi\pi$ elastic scattering ($4m_\pi^2 < s < 16m_\pi^2$). Accordingly, the S -wave parts of A and B , both of which contribute to the $J=0$ amplitude, each contain the factor

$$\exp\left(\frac{s}{\pi} \int_{4m_\pi^2}^{\infty} \frac{\delta_0(s') ds'}{s'(s'-s)}\right), \quad (6.4)$$

where δ_0 can be identified with the S -wave $\pi\pi$ phase shift in the elastic region. In general, however, the A and B amplitudes can be further multiplied by entire functions and still satisfy the unitarity condition (6.3).

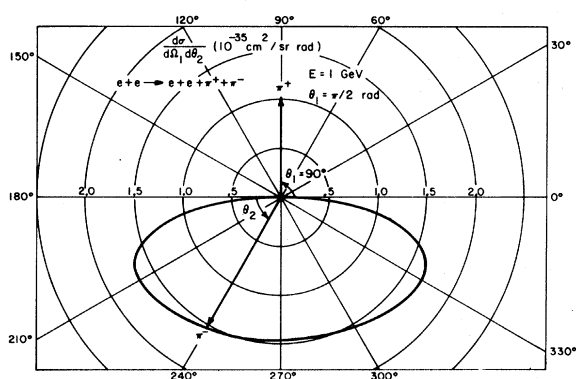


FIG. 8. The cross section $d\sigma/d\Omega_1 d\theta_2$ for the process $e+e \rightarrow e+e+\pi^++\pi^-$ calculated in the equivalent-photon approximation. $E=1$ GeV, $\theta_1=90^\circ$.

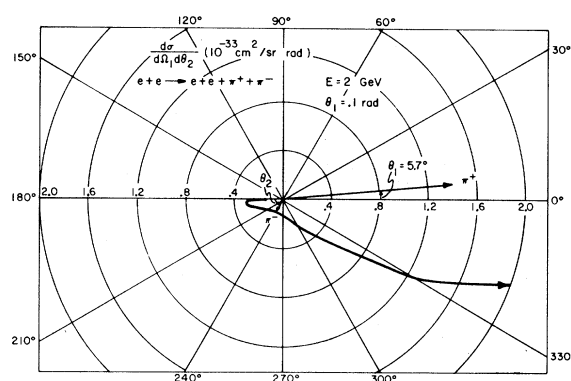


FIG. 9. The cross section $d\sigma/d\Omega_1 d\theta_2$ for the process $e+e \rightarrow e+e+\pi^++\pi^-$ calculated in the equivalent-photon approximation. $E=2$ GeV, $\theta_1=5.7^\circ$.

We also note that the general amplitude will contain additional contributions from all even- l resonances in the $\pi^+\pi^-$ system as well as t and u exchange contributions. Since $\gamma+\gamma \rightarrow \pi^+\pi^-$ is now readily measurable, this process promises to be an ideal new testing ground for various models of hadronic interactions and the search for structure in the $\pi^+\pi^-$ system.

In terms of the A and B functions we have

$$\begin{aligned} \frac{d\sigma_{\gamma\gamma \rightarrow \pi^+\pi^-}}{dt} &= \frac{4\pi}{s(1-4m_\pi^2/s)^{1/2}} \frac{d\sigma}{d\Omega_{c.m.}} \\ &= \frac{2\pi\alpha^2}{s^2} [(1-2r+2r^2)|B|^2 + s^2|A|^2 \\ &\quad - 2rs \text{Re}(A^*B)], \end{aligned} \quad (6.5)$$

where

$$r = \frac{m_\pi^2(k_1 \cdot k_2)}{2(k_1 \cdot q_1)(k_1 \cdot q_2)} = \frac{m_\pi^2 s}{(t-m_\pi^2)(u-m_\pi^2)}. \quad (6.6)$$

Notice that at threshold ($s \rightarrow 4m_\pi^2$, $r \rightarrow 1$) the cross

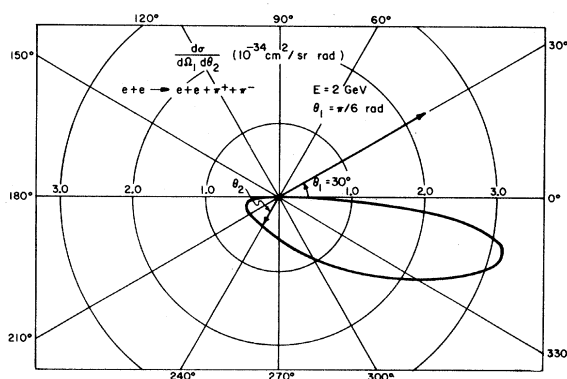


FIG. 10. The cross section $d\sigma/d\Omega_1 d\theta_2$ for the process $e+e \rightarrow e+e+\pi^++\pi^-$ calculated in the equivalent-photon approximation. $E=2$ GeV, $\theta_1=30^\circ$.

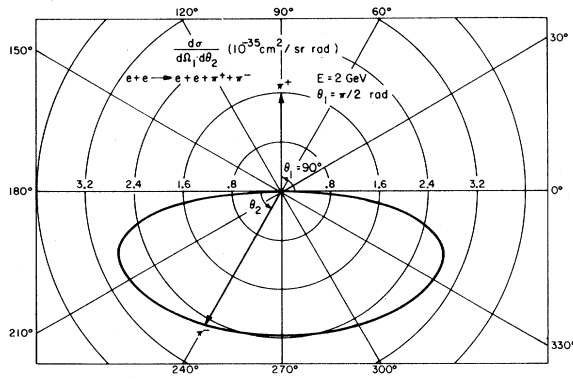


FIG. 11. The cross section $d\sigma/d\Omega_1 d\theta_2$ for the process $e + e \rightarrow e + e + \pi^+ + \pi^-$ calculated in the equivalent-photon approximation. $E = 2$ GeV, $\theta_1 = 90^\circ$.

section (6.5) is proportional to $|B - sA|^2$. This reflects the fact that at threshold the B term yields contributions only to the equal-helicity c.m. amplitude $M_{\lambda_1=\lambda_2}^{c.m.}$, which is the entire contribution of the A term. This amplitude corresponds to oppositely directed angular momentum and is the helicity amplitude which can contribute to the $J=0$ state. At high energies where

$$s \gg 4m_\pi^2 / \sin^2 \theta_{c.m.},$$

i.e., $r \ll 1$, the interference of the A and B terms disappears since then the B term contributes only to the unequal-helicity c.m. amplitude $M_{\lambda_1=-\lambda_2}^{c.m.}$.

B. The σ Contribution

There is a particular interest in understanding the $J=0$ partial-wave contribution to the $\gamma + \gamma \rightarrow \pi^+ + \pi^-$ process since this can yield information on $\pi - \pi$ scattering lengths and s -wave resonances, especially the broad σ or ϵ enhancement near 700 MeV.^{14,29} We shall define the coupling constants

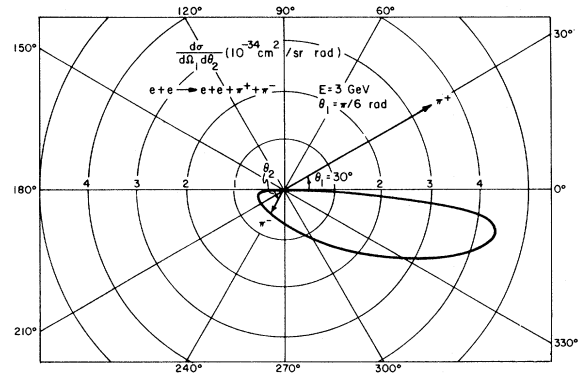


FIG. 13. The cross section $d\sigma/d\Omega_1 d\theta_2$ for the process $e + e \rightarrow e + e + \pi^+ + \pi^-$ calculated in the equivalent-photon approximation. $E = 3$ GeV, $\theta_1 = 30^\circ$.

$g_{\sigma\gamma\gamma}$ and $g_{\sigma\pi\pi}$ in terms of the effective Lagrangians $\mathcal{L}'_1 = (-1/2!)e^2 g_{\sigma\gamma\gamma} F_{\mu\nu} F^{\mu\nu} \phi_\sigma$ and $\mathcal{L}'_2 = -g_{\sigma\pi\pi} \phi_\pi^\dagger \phi_\pi \phi_\sigma$. Obviously, only the A term receives the σ contribution. The product $g_{\sigma\gamma\gamma} g_{\sigma\pi\pi}$ of coupling constants has been estimated by Sarker³⁰ using a superconvergent sum rule for the helicity-flip amplitude of pion Compton scattering.³¹ Taking account of contributions from σ and higher resonances, he obtained a result $2g_{\sigma\gamma\gamma} g_{\sigma\pi\pi} \leq -2.056 \pm 0.6$. (His definition of $g_{\sigma\gamma\gamma}$ differs from ours by a factor of 2.) If one takes only the σ resonance into account in the superconvergent sum rule, one finds $2g_{\sigma\gamma\gamma} g_{\sigma\pi\pi} = -4$. This result can also be obtained very simply by requiring that the forward differential cross section fall faster at high energy than either the Born contribution or the σ contribution (A term) alone. Since $r=1$ for $\theta=0$, this means that we require

$$\lim_{s \rightarrow \infty} (B - sA) = \lim_{s \rightarrow \infty} \left(1 - \frac{-g_{\sigma\gamma\gamma} g_{\sigma\pi\pi}}{2} \frac{s}{s - m_\sigma^2 + i m_\sigma \Gamma_\sigma} \right) = 0, \quad (6.7)$$

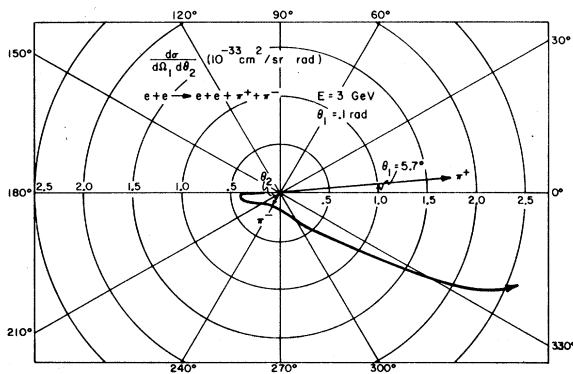


FIG. 12. The cross section $d\sigma/d\Omega_1 d\theta_2$ for the process $e + e \rightarrow e + e + \pi^+ + \pi^-$ calculated in the equivalent-photon approximation. $E = 3$ GeV, $\theta_1 = 5.7^\circ$.

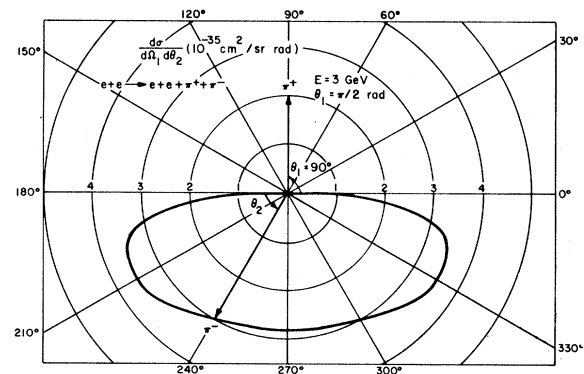


FIG. 14. The cross section $d\sigma/d\Omega_1 d\theta_2$ for the process $e + e \rightarrow e + e + \pi^+ + \pi^-$ calculated in the equivalent-photon approximation. $E = 3$ GeV, $\theta_1 = 90^\circ$.

TABLE III. The cross section $d\sigma/d\Omega_1 d\theta_2$ for the process $e+e \rightarrow e+e+\pi^++\pi^-$ calculated in the equivalent-photon approximation for combinations of $\theta_1 = 5.7^\circ, 30^\circ, 90^\circ$, and $E = 1, 2$, and 3 GeV.

E (GeV)	θ_1 (deg)	θ_2 (deg)																	
		1.15	2.87	11.5	17.2	35.7	60	90	92.9	120	144.3	151.4	157.1	162.8	168.5	174.3	177.1	178.8	
1.0	5.7	1.15	1.95	1.83	1.49	0.88	0.61	0.61	0.62	1.02	2.8	4.7	6.5	10.1	10.5	10.5	10.5	10.4	
	30	0.038	0.23	0.28	0.30	0.29	0.28	0.33	0.35	0.53	0.95	1.14	1.34	1.34	1.39	0.76	0.27	0.041	
	90	0.0040	0.023	0.115	0.147	0.167	0.152	0.143	0.143	0.143	0.152	0.167	0.162	0.147	0.115	0.060	0.023	0.0040	
2.0	5.7	2.0	3.1	2.9	2.4	1.54	1.21	1.34	1.42	2.6	7.7	13.2	17.4	38	3.1	2.0	0.83	0.185	
	30	0.156	0.33	0.44	0.47	0.45	0.45	0.57	0.59	0.95	1.83	2.3	2.7	3.1	3.1	2.0	0.83	0.185	
	90	0.0149	0.061	0.23	0.27	0.28	0.25	0.23	0.23	0.25	0.28	0.29	0.28	0.27	0.23	0.140	0.061	0.0149	
3.0	5.7	2.6	3.8	3.5	2.9	1.94	1.59	1.88	2.0	3.5	10.4	20	25	62	4.4	3.2	1.47	0.32	
	30	0.025	0.103	0.30	0.34	0.35	0.30	0.28	0.28	0.30	0.35	0.35	0.35	0.34	0.30	0.189	0.103	0.025	
	90	0.025	0.103	0.30	0.34	0.35	0.30	0.28	0.28	0.30	0.35	0.35	0.35	0.34	0.30	0.189	0.103	0.025	

which leads to $g_{\sigma\gamma\gamma}g_{\sigma\pi\pi} = -2$.

In Fig. 19 we give representative examples of the effects of $\pi\pi$ hadronic interactions on the total $ee \rightarrow ee\pi^+\pi^-$ cross section. Curves are given for (a) the Born cross section using Eqs. (3.6) and (5.5), and (b) a completely isotropic ($J=0$) contribution from the σ -pole term as defined above plus an isotropic part of the Born amplitude (i.e., $B=1$). The results are shown for the simple form

$$\sigma_{\gamma\gamma \rightarrow \pi^+\pi^-} = \frac{2\pi\alpha^2}{s} \left(1 - \frac{4m_\pi^2}{s}\right)^{1/2} \frac{m_\sigma^4}{(s - m_\sigma^2)^2 + m_\sigma^2\Gamma_\sigma^2}, \quad (6.8)$$

assuming $m_\sigma = 700$ MeV, $\Gamma_\sigma = 400$ and 600 MeV. As is seen from Fig. 19, the cross section including the σ -resonance effect may be larger by a factor of about 2 than the Born cross section. Similar conclusions on the strong-interaction effect has been obtained by Manassah and Matsuda using a harmonic-oscillator model.³²

More definitive information on the $\gamma + \gamma \rightarrow \pi^+ + \pi^-$ process, however, will require measurements of the s dependence (by pion-energy measurements or tagging the scattered electrons) and the angular distributions. Some features of these distributions as seen in the laboratory have been discussed in Sec. V. Tagging of the scattered electrons will be needed to assure complete freedom from the background of one- and two-photon processes.

VII. DEGREE OF NONCOPLANARITY OF THE $\pi^+\pi^-$ PAIR

We have pointed out in Ref. 2 that the $\pi^+\pi^-$ pair produced by the two-photon mechanism is approximately coplanar with the incident beam. This is a

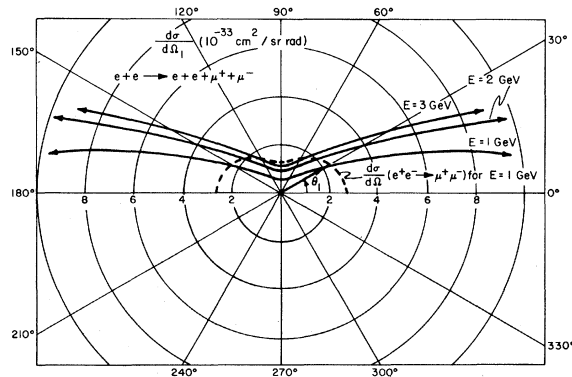


FIG. 15. The cross section $d\sigma/d\Omega_1$ for the process $e+e \rightarrow e+e+\mu^++\mu^-$ calculated in the equivalent-photon approximation for $E = 1, 2$, and 3 GeV. For comparison, the one-photon cross section $d\sigma_{e^+e^- \rightarrow \mu^+\mu^-}/d\Omega_1$ is also shown for $E = 1$ GeV. See Table IV for further information.

simple consequence of the circumstance that the virtual photons are emitted predominantly in the beam direction and hence the plane defined by the momenta of the photons and pions also contains the electron momenta. However, this kinematical restriction is not very strong because of the angular spread of order $(m_e/E)^{1/2}$ of the photon beam [see (3.8)]. As we shall see, the statement that the two-particle production process (e.g., $e+e \rightarrow e+e+\pi^+\pi^-$) produces events "coplanar" with the electron-beam direction is only approximate.

In order to examine this problem let us introduce the momentum \vec{q} of the produced two-body system X :

$$\vec{q} = \vec{q}_1 + \vec{q}_2 = \vec{k}_1 + \vec{k}_2 = -\vec{p}_1' - \vec{p}_2'. \quad (7.1)$$

The angle θ of \vec{q} measured from the initial beam direction is given by

$$\cos\theta = \frac{|\vec{p}_1'| \cos\theta_1' - |\vec{p}_2'| \cos\theta_2'|}{|\vec{q}|}, \quad 0 \leq \theta \leq \frac{1}{2}\pi \quad (7.2)$$

where as before $\cos\theta_1' = \hat{p}_1 \cdot \hat{p}_1'$ and $\cos\theta_2' = \hat{p}_2 \cdot \hat{p}_2'$. We shall call θ the "photon-photon axis angle" in the following. We shall also define the "coplanarity angle ψ " between the two planes, one determined by \vec{q}_1 and \vec{p}_1 and the other by \vec{q}_2 and \vec{p}_2 , by

$$\cos\psi = \frac{(\vec{q}_1 \times \vec{p}_1) \cdot (\vec{q}_2 \times \vec{p}_2)}{|\vec{q}_1 \times \vec{p}_1| |\vec{q}_2 \times \vec{p}_2|}. \quad (7.3)$$

Note that ψ vanishes for $\theta \rightarrow 0$.

Although the coplanarity angle ψ can be defined only for two-particle productions, the photon-photon axis angle θ is general to *all* of the $C=+$ production cross sections, including production of a single hadron such as π^0 or η . It is, therefore, instructive to see how the cross section for π^0 and η production depends on θ . In Table VI we give these cross sections evaluated using the exact for-

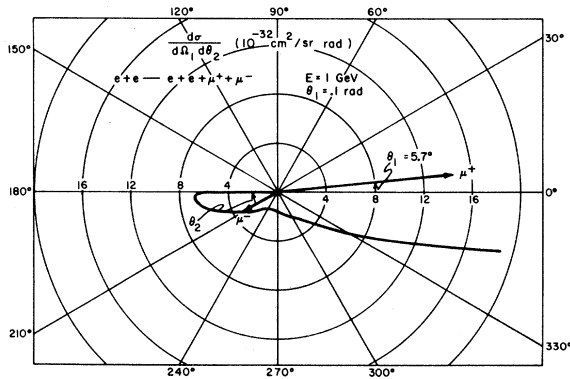


FIG. 16. The cross section $d\sigma/d\Omega_1 d\theta_2$ for the process $e+e \rightarrow e+e+\mu^++\mu^-$ calculated in the equivalent-photon approximation. $E=1$ GeV, $\theta_1=5.7^\circ$.

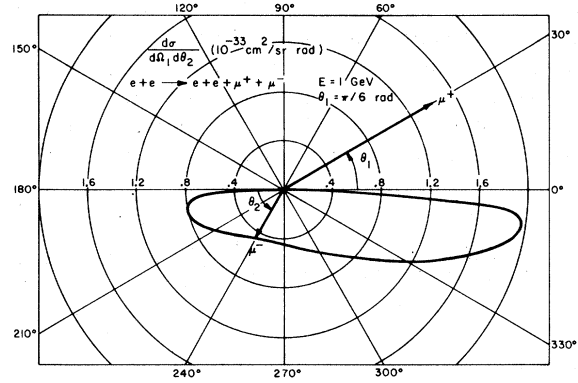


FIG. 17. The cross section $d\sigma/d\Omega_1 d\theta_2$ for the process $e+e \rightarrow e+e+\mu^++\mu^-$ calculated in the equivalent-photon approximation. $E=1$ GeV, $\theta_1=30^\circ$.

mula under the restriction $\theta > \theta_{\min}$ for various cut-off angles θ_{\min} . It is seen that approximately $\frac{1}{2}$ of the total cross section still comes from θ larger than $(m_e/E)^{1/4}$ even though $\frac{1}{2}$ of the emitted photons fall in the much narrower angular region $\theta_\gamma < (m_e/E)^{1/2}$ as is seen from (3.8). It is not difficult to understand this result qualitatively: In (7.1) the longitudinal components (parallel to the electron beam) of \vec{k}_1 and \vec{k}_2 tend to cancel each other whereas the transverse components, which are of order $E(m_e/E)^{1/2}$, may add up, leading to the result $\theta \gg \theta_\gamma$. Furthermore, since this θ dependence of the cross section arises from the spreading of the total momentum $\vec{k}_1 + \vec{k}_2$ of the two-photon system, it will be rather insensitive to the nature of the produced state X . Thus we may expect to find a similar situation in the case of $\pi^+\pi^-$ production, too.

We shall now examine the degree of noncoplanarity of the $\pi^+\pi^-$ pair. For this purpose we have to

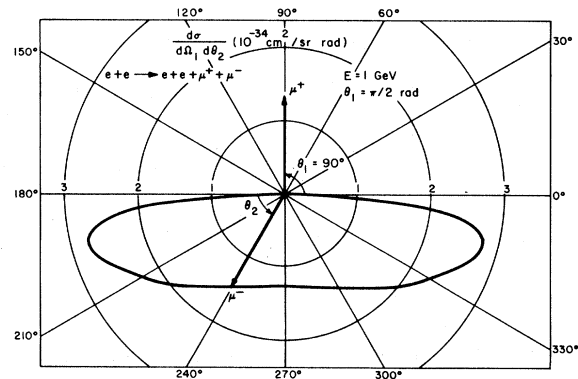


FIG. 18. The cross section $d\sigma/d\Omega_1 d\theta_2$ for the process $e+e \rightarrow e+e+\mu^++\mu^-$ calculated in the equivalent-photon approximation. $E=1$ GeV, $\theta_1=90^\circ$.

calculate a cross section such as $d\sigma/d\psi$. Clearly we have to carry out such a calculation without using the equivalent-photon approximation since the information on the ψ dependence is completely lost in this approximation. To facilitate the computational problem, we have actually calculated the

cross section $d\sigma/d\cos\theta_1 d\cos\theta_2 d\psi$, where θ_1 and θ_2 are angles which π^+ and π^- make with the electron beams.

The cross section $d\sigma/d\cos\theta_1 d\cos\theta_2 d\psi$ is obtained by evaluating the matrix elements $M_{\mu\alpha}$ of (2.10) in perturbation theory. This leads us to

$$\frac{d\sigma}{d\cos\theta_1 d\cos\theta_2 d\psi} = \frac{\pi}{2E^2} \left(\frac{\alpha}{\pi}\right)^4 \int_{m_\pi}^E dW_1 \int_{m_\pi}^E dW_2 \int_{-1}^1 d\cos\theta'_1 \int_{E'_-}^{E'_+} dE'_1 \frac{|\vec{q}_1||\vec{q}_2|}{|\vec{q}_1+\vec{q}_2|\sin\theta_{1+2}\sin\theta'_1\sin\varphi_{1+2}} \sum_{b=\pm 1} \frac{\mathfrak{D}}{(k_1^2 k_2^2)^2}, \quad (7.4)$$

where

$$\begin{aligned} \mathfrak{D} = & \left(2\vec{p}_1 \cdot \vec{p}_2 + \frac{\vec{p}_1 \cdot (k_1 - 2q_1) \vec{p}_2 \cdot (k_1 - q_1 + q_2)}{2k_1 \cdot q_1 - k_1^2} + \frac{\vec{p}_1 \cdot (k_1 - 2q_2) \vec{p}_2 \cdot (k_1 + q_1 - q_2)}{2k_1 \cdot q_2 - k_1^2} \right)^2 \\ & + \frac{1}{4} k_1^2 \left(2\vec{p}_2 + \frac{(k_1 - 2q_1) \vec{p}_2 \cdot (k_1 - q_1 + q_2)}{2k_1 \cdot q_1 - k_1^2} + \frac{(k_1 - 2q_2) \vec{p}_2 \cdot (k_1 + q_1 - q_2)}{2k_1 \cdot q_2 - k_1^2} \right)^2 \\ & + \frac{1}{4} k_2^2 \left(2\vec{p}_1 + \frac{(k_1 - q_1 + q_2) \vec{p}_1 \cdot (k_1 - 2q_1)}{2k_1 \cdot q_1 - k_1^2} + \frac{(k_1 + q_1 - q_2) \vec{p}_1 \cdot (k_1 - 2q_2)}{2k_1 \cdot q_2 - k_1^2} \right)^2 \\ & + \frac{1}{16} k_1^2 k_2^2 \left(16 + \frac{4(k_1 - 2q_1) \cdot (k_1 - q_1 + q_2)}{2k_1 \cdot q_1 - k_1^2} + \frac{(k_1 - 2q_1)^2 (k_1 - q_1 + q_2)^2}{(2k_1 \cdot q_1 - k_1^2)^2} \right. \\ & \quad + \frac{4(k_1 + q_1 - q_2) \cdot (k_1 - 2q_2)}{2k_1 \cdot q_2 - k_1^2} + \frac{(k_1 + q_1 - q_2)^2 (k_1 - 2q_2)^2}{(2k_1 \cdot q_2 - k_1^2)^2} \\ & \quad \left. + \frac{2(k_1 - 2q_1) \cdot (k_1 - 2q_2) (k_1 - q_1 + q_2) \cdot (k_1 + q_1 - q_2)}{(2k_1 \cdot q_1 - k_1^2)(2k_1 \cdot q_2 - k_1^2)} \right), \quad (7.5) \end{aligned}$$

W_1, W_2 are pion energies defined by (5.10), (5.12), and

$$\begin{aligned} \cos\theta_{1+2} &= \frac{\vec{p}_1 \cdot (\vec{q}_1 + \vec{q}_2)}{|\vec{p}_1||\vec{q}_1 + \vec{q}_2|}, \\ \cos\beta &= \frac{(2E - W_1 - W_2)^2 - |\vec{q}_1 + \vec{q}_2|^2 - 2E'_1(2E - W_1 - W_2)}{2|\vec{p}_1||\vec{q}_1 + \vec{q}_2|}, \quad (7.6) \end{aligned}$$

$$\cos\varphi_{1+2} = \frac{\cos\beta - \cos\theta'_1 \cos\theta_{1+2}}{\sin\theta'_1 \sin\theta_{1+2}},$$

$$E'_\pm = \frac{(2E - W_1 - W_2)^2 - |\vec{q}_1 + \vec{q}_2|^2}{2[2E - W_1 - W_2 + |\vec{q}_1 + \vec{q}_2| \cos(\theta'_1 \pm \theta_{1+2})]}.$$

The summation in (7.4) is over the possibilities $b = +1$ and -1 in

$$\begin{aligned} \varphi_1 &= \varphi_{1+2} - b \cos^{-1} \left(\frac{|\vec{q}_1|^2 \sin^2\theta_1 + |\vec{q}_1 + \vec{q}_2|^2 \sin^2\theta_{1+2} - |\vec{q}_2|^2 \sin^2\theta_2}{2|\vec{q}_1| \sin\theta_1 |\vec{q}_1 + \vec{q}_2| \sin\theta_{1+2}} \right), \\ \varphi_2 &= \varphi_{1+2} + b \cos^{-1} \left(\frac{|\vec{q}_2|^2 \sin^2\theta_2 + |\vec{q}_1 + \vec{q}_2|^2 \sin^2\theta_{1+2} - |\vec{q}_1|^2 \sin^2\theta_1}{2|\vec{q}_2| \sin\theta_2 |\vec{q}_1 + \vec{q}_2| \sin\theta_{1+2}} \right), \quad (7.7) \end{aligned}$$

where φ_1 and φ_2 are the azimuthal angles of \vec{q}_1 and \vec{q}_2 , respectively, with respect to the plane containing \vec{p}'_1 and the incident beams.

In Fig. 20 and Table VII we show the ψ dependence of the cross section $d\sigma/d\cos\theta_1 d\cos\theta_2 d\psi$ for typical

angles $\theta_1 = 90^\circ, \theta_2 = 60^\circ; \theta_1 = 30^\circ, \theta_2 = 120^\circ; \theta_1 = 5.7^\circ, \theta_2 = 157^\circ; \theta_1 = 5.7^\circ, \theta_2 = 174.3^\circ$; all at $E = 1$ GeV.³³ It is seen that all these curves behave as ψ^{-1} for large ψ [$\psi > 2^\circ \approx (m_e/E)^{1/2}$]. Similar behavior is likely to be observed for other combinations of θ_1

TABLE IV. The cross section $d\sigma/d\Omega_1$ for the process $e+e \rightarrow e+e+\mu^++\mu^-$ calculated in the equivalent-photon approximation for $E=1, 2,$ and 3 GeV. The one-photon cross section $d\sigma_{e^+e^- \rightarrow \mu^+\mu^-}/d\Omega_1$ is also given for $E=1$ GeV.

E (GeV)	θ_1 (deg)							
	1.0	5.7	11.5	17.2	22.9	30	60	90
	$d\sigma_{ee \rightarrow ee\mu^+\mu^-}/d\Omega_1$ (10^{-33} cm ² /sr)							
1.0	22	15.7	8.6	5.5	3.5	2.3	0.75	0.55
2.0	121	52	20	10.8	6.4	3.8	1.28	0.89
3.0	290	82	28	13.8	8.3	4.9	1.56	1.13
	$d\sigma_{e^+e^- \rightarrow \mu^+\mu^-}/d\Omega_1$ (10^{-33} cm ² /sr)							
1.0	2.6	2.6	2.5	2.5	2.4	2.3	1.62	1.30

and θ_2 . If we integrate the cross section

$$d\sigma/d\cos\theta_1 d\cos\theta_2 d\psi$$

over ψ using the curves of Fig. 20, the result can be compared with $d\sigma^{(0)}/d\Omega_1 d\theta_2$ of (5.11) obtained in the equivalent-photon approximation where the superscript (0) refers to the equivalent-photon approximation as in (3.2). Note that the $1/\psi$ behavior for small ψ leads to a logarithmic factor $\ln(E/m_e)$ in $\int (d\sigma/d\cos\theta_1 d\cos\theta_2 d\psi) d\psi$. Note also that the relation between this integral and $d\sigma^{(0)}/d\Omega_1 d\theta_2$ is not straightforward because certain averaging over the azimuthal angles has to be made in deriving the latter as is seen from (A5). Nevertheless this integral and $(2\pi/\sin\theta_2)d\sigma^{(0)}/d\Omega_1 d\theta_2$ are expected to be of the same order of magnitude. The results of graphic integration using the curves of Fig. 20 are shown in Table VIII. It is seen that the exact results are in fact in rough agreement with (although somewhat smaller than) the equivalent-photon results. Further work is in progress to determine whether or not the exact *total* cross section is smaller than the equivalent-photon result in the case of $\pi^+\pi^-$ production.

The most significant feature seen from Fig. 20 and Table VIII is that pion pairs produced by the

two-photon mechanism are much more noncoplanar than what is implied by the quantity $(m_e/E)^{1/2}$. Although we only give results for four sets of θ_1, θ_2 , the strong deviation from the coplanarity is seen to be a general feature judging from the almost identical shape of curves of Fig. 20 for different values of θ_1 and θ_2 . It is not difficult to understand this if we recall that the largeness of the coplanarity angle ψ is closely related to (and in fact more or less determined by) the largeness of the photon-photon axis angle θ described earlier.

From Table VIII it is seen that 40–50% of all pion pairs are emitted with the coplanarity angle ψ greater than 12° . If we assume that this result holds for other pairs of θ_1 and θ_2 as well, then a sizable fraction of two-charged-particle events classified as multiple production events in Ref. 13 may have to be reclassified as the pion (or muon) pairs produced by the two-photon mechanism.

VIII. MISCELLANEOUS TOPICS

A. Other Higher-Order Contributions

In addition to the diagrams for the two-photon process which produced $C=+$ final states, the diagrams shown in Fig. 1(b) for $C=-$ states will also contribute logarithmically increasing total cross sections in e^+e^- collisions.³ The equivalent-photon method applied to one electron (or positron) leg gives the leading contribution for $m_e/E \ll 1$:

$$d\sigma_{ee \rightarrow eeX(C=-)} = \frac{2\alpha}{\pi} \left(\ln \frac{E}{m_e} \right) \int \frac{d\omega}{\omega} N(\omega) d\sigma_{\gamma e \rightarrow eX}, \quad (8.1)$$

where $d\sigma_{\gamma e \rightarrow eX}$ is the differential cross section for a real photon in collision with an electron to produce the state X . This cross section is finite for $m_e \rightarrow 0$ (provided X is not the state e^+e^-) and hence the cross section (8.1) is only singly logarithmic in E/m_e . Of course, the actual magnitude of this cross section must be determined by an explicit calculation, a problem to be settled before long. We note that, in principle, this $C=-$ production cross section can be completely calculated

TABLE V. The cross section $d\sigma/d\Omega_1 d\theta_2$ for the process $e+e \rightarrow e+e+\mu^++\mu^-$ calculated in the equivalent-photon approximation for $\theta_1=5.7^\circ, 30^\circ, 90^\circ$, and $E=1$ GeV.

θ_1 (deg)	θ_2 (deg)												
	1.15	2.9	11.5	17.2	35.7	60	92.9	120	144.3	151.4	157.1	162.8	177.1
	$d\sigma_{ee \rightarrow ee\mu^+\mu^-}/d\Omega_1 d\theta_2$ (10^{-33} cm ² /sr rad)												
5.7	4.0	6.9	6.1	4.9	2.9	1.71	1.78	2.7	5.7	6.8	10.0	15.4	61
30	0.133	0.49	0.79	0.79	0.60	0.46	0.45	0.59	0.38	1.20	1.41	1.71	0.70
90	0.0123	0.066	0.27	0.27	0.21	0.144	0.124	0.144	0.21	0.23	0.25	0.27	0.066

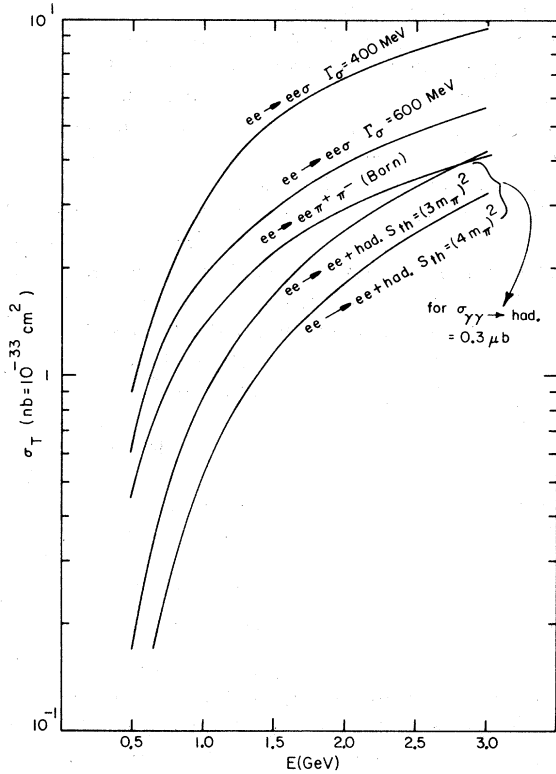


FIG. 19. Effects of hadronic interactions on the total two-photon cross sections. Curves are given for (a) the Born cross section, (b) a completely isotropic ($J=0$) contribution from the σ -pole term plus an isotropic part of the Born amplitude (i.e., $B=1$) with $m_\sigma=700$ MeV, $\Gamma_\sigma=400$ and 600 MeV, and (c) estimated cross sections for multihadron production with assumed threshold $s_{th}=(3m_\pi)^2$ and $(4m_\pi)^2$.

from the knowledge of the one-photon process (1.2).

We should also emphasize that contributions of other higher-order diagrams for hadron production in which the incident e^+ and e^- beams annihilate decrease with energy as in the one-photon process (1.2). Examples are the order- α radiative correction to $e^+ + e^- \rightarrow \gamma^* \rightarrow X$ including the emission of hard photons,³⁴ and the process³⁵

$$e^+ + e^- \rightarrow \gamma^* + \gamma^* \rightarrow X. \quad (8.2)$$

B. Remarks About Purely Leptonic Processes

Purely leptonic processes $e+e \rightarrow e+e+e^++e^-$ and $e+e \rightarrow e+e+\mu^++\mu^-$ can serve as checks on the fourth-order quantum-electrodynamics (QED) calculation (analogous to the trident experiments) or as normalization checks on the two-photon mechanism. They have to be understood especially well because the large magnitude of their total cross sections can cause serious background problems to the other colliding-beam processes,

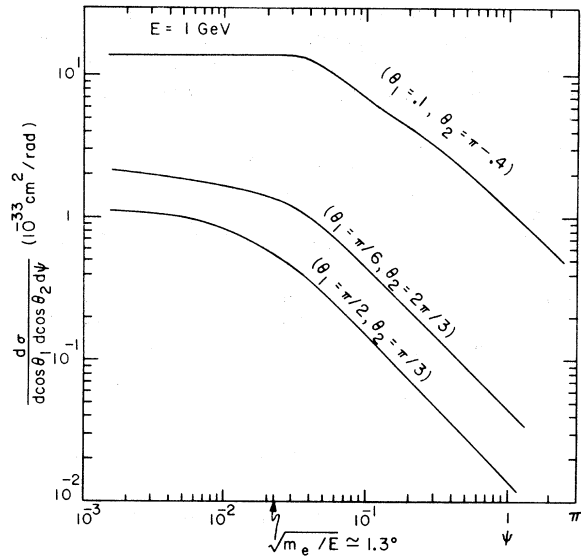


FIG. 20. Dependence of the cross section $d\sigma/d\cos\theta_1 d\cos\theta_2 d\psi$ on the coplanarity angle ψ for typical angles $\theta_1=90^\circ$, $\theta_2=60^\circ$; $\theta_1=30^\circ$, $\theta_2=120^\circ$; $\theta_1=5.7^\circ$, $\theta_2=157^\circ$. $E=1$ GeV.

if the scattered electrons in the final state are not detected.

There are three main factors that influence the experimental counting rates of these lepton-pair-production processes.

(1) The experiment will set a threshold on the minimum invariant mass $s_{min}^{1/2}$ of the lepton pair that can be observed. Accordingly, the measured cross sections are reduced by the substitution of s_{min} for the threshold value of the s integration in (3.6), for example. Thus, the measured cross sections for the case when the produced electron-positron pairs are detected are of order $(\alpha^4/s_{min}) \times [\ln(E/m_e)]^2 \ln(E^2/s_{min})$ rather than the theoretical cross section $\sim (\alpha^4/m_e^2) [\ln(E/m_e)]^3$.

(2) The experiment sets a limit on the minimum angle of the detected particles of the produced system X . As we have seen in Sec. V, this is not a particularly severe effect when $d\sigma_{\gamma\gamma \rightarrow X}$ is nearly isotropic in the photon-photon center-of-mass system as in the case $X=\pi^+\pi^-$ (~50% efficiency loss in this case). However, in the case of $\mu^+\mu^-$ (or e^+e^-) production, the effect of the angular cutoff will be considerable. In general, enhancement factors of $\ln(4E^2/s_{min})$ are missing in the theoretical cross section integrated over wide-angle phase space. In addition, for the case of the electron pair-production processes, $e+e \rightarrow e+e+e^++e^-$, $e+e \rightarrow e+e+e^++e^-+e^++e^-$,³⁶ etc., the requirement that at least one final-state electron be detected at a wide angle $\theta > \theta_{min} \gg m_e/E$, eliminates the inverse dependence of the total rate on m_e^2 .

TABLE VI. π^0 and η production cross sections calculated with the cutoff $\theta > \theta_{\min}$, where θ is the photon-photon axis angle defined by (7.2). $E = 1$ GeV.

X	θ_{\min} (rad)				
	0	$m_e/E = 0.511 \times 10^{-3}$	$(m_e/E)^{1/2} = 0.0226$	$(m_e/E)^{1/4} = 0.150$	$(m_e/E)^{1/8} = 0.388$
	$\sigma_{ee \rightarrow eeX}^{\text{exact}}(\theta > \theta_{\min})$ (10^{-34} cm 2)				
π^0	5.4	5.3	4.2	2.6	1.63
η	3.0	3.0	2.5	1.57	1.00

(3) As we have discussed in Sec. V, the two-particle production cross sections are dominated by events in which the produced particle pair is noncollinear but roughly coplanar with the beam direction. In general, a considerable fraction of the events are noncoplanar (see Sec. VII) and thus this criterion is not sufficient to distinguish the two-particle production through the two-photon mechanism and multihadron ($n > 2$) production through the one-photon annihilation mechanism. The large event rates for $e+e \rightarrow e+e+e^++e^-$ and $e+e \rightarrow e+e+\mu^++\mu^-$ can make these processes an especially serious background for multihadron production without complete particle identification. In general, the necessity for experimental arrangements which have provision for detecting and possibly tagging the scattered electrons seems to be unavoidable.

C. Estimate of Multihadron Production in the Two-Photon Process

It is desirable to have at least a rough estimate of the multihadron production cross section via the two-photon process. We present here a simple argument based on the equivalent-photon method and a duality-type approach to $\sigma_{\gamma\gamma \rightarrow \text{hadrons}}$.³⁷

The general components of the total cross section $\sigma_{\gamma\gamma \rightarrow \text{hadrons}}$ consist of

- the contribution of narrow $C=+$ resonances (π^0 , η , η' , etc.) described in Sec. IV,
- two-pion production starting at the threshold

$s_{\text{th}} = (2m_\pi)^2$ modulated by the even l resonances and enhancements in the π - π system,

(c) the contribution of resonances which decay into other hadronic systems,

(d) and finally a nearly flat asymptotic component which may be estimated by factorization of the cross section at high energy⁴ (universal Pom-eranchukon coupling) or ρ dominance to be

$$\sigma_{\gamma\gamma \rightarrow \text{had}}^{\text{asympt}} \cong \frac{(\sigma_{\gamma p}^{\text{asympt}})^2}{\sigma_{pp}^{\text{asympt}}} \cong 0.3 \mu\text{b} \quad (8.3)$$

for large s .

From a duality point of view we can consider $\sigma_{\gamma\gamma \rightarrow \text{had}}(s)$ as being essentially equal to $\sigma_{\gamma\gamma \rightarrow \text{had}}^{\text{asympt}}(s)$ with the $C=+$ resonances modulating the asymptotic value. Thus, very roughly, the multibody cross section might be expected to average out to $0.3 \mu\text{b}$ starting at a threshold s_{th} for s of order $(3m_\pi)^2$ or $(4m_\pi)^2$. We thus estimate

$$\begin{aligned} \sigma_{ee \rightarrow ee+X}(\text{anything but } 2\pi) &\cong 2 \left(\frac{\alpha}{\pi}\right)^2 \left(\ln \frac{E}{m_e}\right)^2 \int_{s_{\text{th}}}^{4E^2} \frac{ds}{s} f\left(\frac{\sqrt{s}}{2E}\right) \sigma_{\gamma\gamma \rightarrow \text{had}}^{\text{asympt}} \\ &\cong 2 \left(\frac{\alpha}{\pi}\right)^2 \left(\ln \frac{E}{m_e}\right)^2 (0.3 \mu\text{b}) \\ &\quad \times [(\ln y_0)^2 + (\ln y_0)(3 + 2y_0 + \frac{1}{4}y_0^2) \\ &\quad + (1 - y_0)(\frac{37}{8} + \frac{5}{8}y_0)], \end{aligned} \quad (8.4)$$

with $y_0 = s_{\text{th}}/4E^2$. The results for the total cross section are plotted in Fig. 19. The cross section

TABLE VII. The cross section $d\sigma/d\cos\theta_1 d\cos\theta_2 d\psi$ for the process $e+e \rightarrow e+e+\pi^+\pi^-$, where ψ is the coplanarity angle defined by (7.3). $E = 1$ GeV.

(θ_1, θ_2) (deg)	ψ (deg)						
	0.1	0.5	1.0	5.0	12	30	60
	$d\sigma_{ee \rightarrow ee\pi^+\pi^-}^{\text{exact}}/d\cos\theta_1 d\cos\theta_2 d\psi$ (10^{-33} cm 2 /rad)						
(5.7, 174.3)	150	144	164	102	59	26	5.0
(5.7, 157.1)	13.7	11.4	12.5	7.5	4.3	2.2	0.57
(30, 120)	2.0	1.45	1.27	0.46	0.23	0.093	0.0172
(90, 60)	1.11	0.80	0.47	0.188	0.073	0.034	0.0064

TABLE VIII. The cross section $\int (d\sigma/d\cos\theta_1 d\cos\theta_2 d\psi) d\psi$ for the process $e+e \rightarrow e+e+\pi^+\pi^-$ obtained by graphic integration of curves of Fig. 20 where ψ is the coplanarity angle defined by (7.3). $E=1$ GeV. Integrations are carried out for $\psi > 0^\circ$ and $\psi > 12^\circ$. For comparison the cross sections $d\sigma/d\cos\theta_1 d\cos\theta_2$ calculated in the equivalent-photon approximation are also shown.

	(θ_1, θ_2) (deg)			
	(5.7, 174.3)	(5.7, 157.1)	(30, 120)	(90, 60)
	$d\sigma_{ee \rightarrow ee\pi^+\pi^-}/d\cos\theta_1 d\cos\theta_2$ (10^{-33} cm 2)			
Exact	55	4.7	0.26	0.099
Exact ($\psi > 12^\circ$)	34	2.2	0.121	0.040
e.p. approx.	66	10.4	0.38	0.110
<u>Exact ($\psi > 12^\circ$)</u>	0.62	0.47	0.46	0.40
Exact				
<u>Exact</u>	0.83	0.45	0.68	0.90
e.p. approx.				

for producing three or more hadrons is seen to be comparable in magnitude to the two-pion production cross section discussed in Sec. VI.

We may also obtain a simple estimate of the cross section for the process $e+e \rightarrow e+e+\rho^0+\rho^0 \rightarrow e+e+\pi^++\pi^--+\pi^++\pi^-$ via ρ dominance. For $s > (2m_\rho)^2$ we expect

$$\begin{aligned} \sigma_{\gamma\gamma \rightarrow \rho\rho} &\cong (e/2\gamma_\rho)^4 \sigma_{\rho\rho \rightarrow \rho\rho} \\ &\sim \left(\frac{1}{300}\right)^2 (10 \text{ mb}) \sim 0.1 \mu\text{b}. \end{aligned} \quad (8.5)$$

This gives $\sigma_{ee \rightarrow ee\rho\rho} \sim 2 \times 10^{-34}$ cm 2 at 2 GeV per beam. For other approaches see Refs. 38 and 39.

D. Detection of Electrons Scattered into Large Angles

Throughout this paper we have considered the process $e+e \rightarrow e+e+X$ in which the electrons in the final state are either not detected or detected only if they are scattered into small forward cones.⁴⁰ However, in the typical arrangement of colliding-beam experiments in which all charged particles emitted at large angles are detected, there would be no particular complication in detecting one or both of the electrons scattered into large angles in addition to the produced particles.

Although the cross section $d\sigma_{ee \rightarrow eeX}$ is in general small for large $k_1^2 = (p_1 - p_1')^2$ for any specific state X ,⁴¹ it might be large enough to be observable if it is summed over all possible final states X . Thus, it will be of considerable interest to obtain an estimate of the cross section for observing one electron scattered with a relatively large momentum transfer while observing the produced particle (whatever they are) at the same time. In this circumstance we can treat the second electron beam by the equivalent-photon method and re-

gard it as a superposition of photon targets. From this point of view our process may be called the "deep-inelastic electron-photon scattering," since it has features quite similar to the familiar deep-inelastic electron-proton scattering.⁴² Details of this problem are discussed in a separate paper.¹⁷

E. Application to Nonleptonic Collisions

The equivalent-photon formalism can also be used to obtain an estimate of the magnitude of two-photon processes in high-energy electron-hadron and hadron-hadron collisions. As viewed from the center-of-mass frame, the dominant high-energy contribution again is obtained from Eq. (3.3) using the approximate equivalent-photon spectrum for each incident charged particle. For the case of proton-proton collisions, the dominant contribution to the cross section for the process $p+p \rightarrow p+p+X$ suffers at least from a factor

$$\left(\ln \frac{E_p}{m_p}\right)^2 / \left(\ln \frac{E_e}{m_e}\right)^2 \quad (8.6)$$

compared to the corresponding electron-electron-induced process. For $E_p = 28$ GeV available at the CERN intersecting rings, this ratio is about $\frac{1}{8}$ compared to the electron-electron collision at $E_e = 2$ GeV. Aside from the production of low-invariant-mass electron pairs (which in fact contributes ~ 1.5 mb to the pp total cross section⁴³), the two-photon processes are of negligible importance; in particular, this process gives cross sections which are of order α^2 smaller than the Drell-Yan⁴⁴ hard-parton annihilation cross section for producing large-invariant-mass electron or muon pairs. Note that at large invariant pair mass (e.g., the mass of the muon pair) the minimum photon mass

$$|k^2|_{\min} = \frac{m_p^2(E-E')^2}{EE'} + O\left(\frac{m_p^4}{E^2}\right) \\ = O\left(\frac{m_p^2 m_{\mu^+ \mu^-}}{EE'}\right) \quad (8.7)$$

is not negligible so that form-factor suppression is also important. Similar remarks apply to the cross section for the process

$$p + U \rightarrow \mu^+ + \mu^- + \text{anything} \quad (8.8)$$

measured in the Columbia-BNL experiment.⁴⁵ Because of the form-factor effects, the coherence of the uranium target plays no role, and the process can be again viewed as a p - p collision in the center-of-mass frame. The rates for the two-photon process are negligible compared with what is observed.

In the case of inelastic e - p collisions, the two-photon process producing lepton pairs corresponds to the usual trident process,

$$e + p \rightarrow e + e^+ + e^- + p. \quad (8.9)$$

Although *total* cross sections for electron tridents are large and of order $(1/m_e^2)Z^2\alpha^4[\ln(E/m_e)]^2$, the contribution to the differential cross section at normal wide electron angles ($|k^2| \gg m_e^2$) has only logarithmic dependence on the electron mass m_e and is a small standard component of the radiative-correction analysis in deep-inelastic e - p scattering experiments.

In Table IX a comparison of the trident contribution with $d\sigma_{ep \rightarrow a11}/dE'd\Omega'$ with the SLAC experimental results⁴⁶ are given. The trident cross section was obtained by numerical integration over the complete differential cross section computed by Brodsky and Ting.⁴⁷ The calculation assumes a static nucleon target with the usual elastic form factor. The contribution is seen to be negligible

TABLE IX. Electron-trident background to inelastic electron scattering. The trident contribution is obtained by numerical integration of the complete differential cross section $e^- + p \rightarrow e^- + e^+ + e^- + p$ over the phase space of the undetected pair. Exchange diagrams are included, but the proton is treated as a static target with a form factor. See Ref. 47. The last column gives the measured values of $d\sigma_{ep \rightarrow a11}/dE'd\Omega'$.

E (GeV)	E' (GeV)	θ' (deg)	$\frac{d\sigma}{dE'd\Omega'}$ (trident) $\left(\frac{\text{nb}}{\text{GeV sr}}\right)$	Measured rate $\left(\frac{\text{nb}}{\text{GeV sr}}\right)$
5	3	1.5	1.0×10^3	0.5×10^6
5	3.3	1.5	0.42×10^3	0.4×10^6
19.5	10.27	6	0.02	1.0×10^2
19.5	10.27	10	0.12×10^{-3}	9.0

beyond $\theta'_e = 1.5^\circ$.

IX. CONCLUDING REMARKS

In this paper we have studied production of hadrons and leptons by the two-photon mechanism in high-energy colliding-beam experiments. This mechanism will provide efficient means for the study of $C=+$ hadronic states and will play a role equal in importance and complementary to that of the one-photon-annihilation mechanism in the case of the $C=-$ states. In order to extract information on $C=+$ and $C=-$ states from high-energy colliding-beam experiments, however, we must be able to separate and identify these states experimentally. We shall examine this problem briefly.

Let us first discuss the $\pi^+\pi^-$ production in an e^+e^- collision. In this case pions may be produced by both e^+e^- -annihilation and two-photon mechanisms. Pions produced by the first mechanism carry the energy E of the incident beam and are strongly constrained to be collinear and coplanar. On the other hand, pions produced by the second mechanism have lower energies and only few of them come out in a collinear fashion as was shown in Sec. V. In the energy range $0.9 \leq E \leq 1.2$ GeV covered by the colliding-beam experiments at Frascati,¹³ the latter pions therefore constitute a small background which can be easily distinguished by accurate energy measurements. Detection of scattered electrons, although desirable, is not absolutely necessary to separate the two processes. At higher beam energies, which will soon be available, however, the two-photon mechanism will inevitably become the dominant process. Collinearity of a pion pair will no longer be a sufficient criterion. For positive identification of two processes, besides accurate measurement of energy and momentum of the produced pion, detection of at least one of the scattered electrons is highly desirable.

As far as the study of the $C=+$ state of $\pi^+\pi^-$ is concerned, the e^-e^- collision has an advantage over the e^+e^- collision in that it has no e^+e^- annihilation channel. In this case the $\pi^+\pi^-$ pair is produced mostly by the two-photon process and the production of $\pi^+\pi^-$ in the $C=-$ state by the bremsstrahlung process [Fig. 1(b)] is expected to be a minor background. In this connection, we should recall that those events in which both electrons are detected at small forward angles [$\theta \lesssim (m_e/E)^{1/2}$] allow a particularly clean interpretation in terms of $C=+$ production via the two-photon mechanism since the contribution of the $C=-$ bremsstrahlung [Fig. 1(b)] and contributions from nonzero photon mass become negligible in this region.³ Of course, the last remark applies to the e^+e^- collision, too.

The situation is enormously more complicated in the case of the multihadron production ($n \geq 3$). Even in the energy range $0.9 \leq E \leq 1.2$ GeV in which the Frascati experiments observed a surprisingly large number of multiparticle production events,¹³ its interpretation is by no means simple because forward-scattered electrons in the final state are presently undetected and both identification and energy measurement of the produced particles are not accurate enough to eliminate ambiguities. In addition to complications from the copious lepton pair production discussed in Secs. V and VIII B, the predicted rate for hadron production by the two-photon mechanism would exceed 3×10^{-33} cm² at $E = 1$ GeV. As was shown in Sec. VII, a substantial fraction of these events can simulate the multihadron production by the one-photon mechanism under the present experimental conditions. Also, additional background processes involving $C = -$ production [Fig. 1(b)] and the hard-photon production process³⁴ have to be taken into account.

We believe that in most future colliding-beam experiments it will not be sufficient to have accurate measurements of energies and momenta of produced hadrons. Detection of either or both of the scattered electrons in addition to produced particles will be required in order to identify and separate the one-photon and two-photon processes. There is no doubt that development of techniques for detection and possibly energy tagging of forward-scattered electrons is crucial for the success of colliding-beam physics.

Finally we shall indicate some new areas of investigation which will become feasible once such detection techniques are available.

(1) The detailed investigation of photon-photon annihilation into a $C = +$ pair of charge-conjugate particles as a function of center-of-mass energy, momentum transfer, and (eventually) spacelike photon mass. These processes will provide abundant information on the analytically continued Compton scattering amplitude and serve as testing grounds of various theoretical ideas.^{32,39}

(2) Measurement of the two-photon coupling of various narrow resonances.¹² A particularly interesting consequence of such a measurement is the possibility that predictions of symmetry schemes may be subjected to a severe experimental test. An example is the 2γ decay mode of the X^0 or $\eta'(960)$ meson. A prediction of the decay rate from broken SU(3) is⁴⁸

$$\Gamma_{\eta' \rightarrow \gamma\gamma} = 6 \text{ keV}. \quad (9.1)$$

This leads to a prediction for the cross section of the process

$$e + e \rightarrow e + e + \eta' \rightarrow \pi^+ + \pi^- + \pi^+ + \pi^- + \pi^0, \text{ etc.}, \quad (9.2)$$

of approximately the same magnitude at $E > 1.2$ GeV as that of the η -meson production shown in Fig. 4. An anomalously large coupling of the η' to two photons compared with (9.1) could yield a substantial number of events with four charged-particle tracks even at present Frascati energies. It will be instructive to derive an upper limit of the partial decay width $\Gamma_{\eta' \rightarrow \gamma\gamma}$ from the preliminary data reported by the Frascati groups.⁴⁹ In parallel with (4.4) we obtain

$$\begin{aligned} \sigma_{ee \rightarrow ee \eta'} &\simeq 16 \alpha^2 \Gamma_{\eta' \rightarrow \gamma\gamma} [\ln(E/m_e)]^2 f(m_{\eta'}/2E) m_{\eta'}^{-3} \\ &= (2.5 \times 10^{-35} \text{ cm}^2) \times \Gamma_{\eta' \rightarrow \gamma\gamma} \end{aligned} \quad (9.3)$$

for $E = 1$ GeV, and with $\Gamma_{\eta' \rightarrow \gamma\gamma}$ in keV. On the other hand, we have

$$\sigma_{ee \rightarrow ee 2\pi^+ 2\pi^- \pi^0} \geq \sigma_{ee \rightarrow ee \eta'} R_{\eta' \rightarrow \eta \pi^+ \pi^-} R_{\eta \rightarrow \pi^+ \pi^- \pi^0} \quad (9.4)$$

and

$$\begin{aligned} \sigma_{ee \rightarrow ee \pi^+ \pi^- \text{ neutrals}} &\geq \sigma_{ee \rightarrow ee \eta'} (R_{\eta' \rightarrow \eta \pi^+ \pi^-} R_{\eta \rightarrow \text{neutrals}} \\ &+ R_{\eta' \rightarrow \eta \pi^0 \pi^0} R_{\eta \rightarrow \pi^+ \pi^- \pi^0} + R_{\eta' \rightarrow \rho \gamma} R_{\rho \rightarrow \pi^+ \pi^-}), \end{aligned} \quad (9.5)$$

R being various branching ratios of the η' and η decays. Using the preliminary data from Frascati,⁴⁹ the present particle data,²⁰ and Eqs. (9.3)–(9.5), we obtain the upper limit

$$\Gamma_{\eta' \rightarrow \gamma\gamma} \leq 600 \pm 300 \text{ keV}. \quad (9.6)$$

This value is three times larger than the upper limit derived from the present particle data,²⁰ $\Gamma_{\eta' \rightarrow \gamma\gamma} < (190 \pm 120)$ keV. This is of course not surprising since the Frascati data may contain many non- η' events. In fact, it does not seem to be too difficult to remove most non- η' events from the data and improve the upper limit (9.6). For this purpose it is of course desirable to measure E_X and \vec{p}_X , the energy and momentum of the produced system X . Then we can use $s = E_X^2 - \vec{p}_X^2$ to reject non- η' events. However, complete information on E_X and \vec{p}_X may not be necessary in some cases. For instance, if E_X is close to the total energy $2E$, the process is likely to be a one-photon process and X is not η' . Also, if \vec{p}_X is very small, a crude estimate of E_X will suffice to exclude non- η' events.

(3) The extensive investigation of the total hadron production cross section by the two-photon mechanism. Of particular interest will be the deep-inelastic electron-photon scattering as a probe into

the hadronic structure of the photon.¹⁷

ACKNOWLEDGMENTS

We should like to thank Dr. S.D. Drell, Dr. J.D. Bjorken, Dr. D.R. Yennie, Dr. C.H. Llewellyn Smith, and Dr. J.J. Sakurai for helpful discussions.

APPENDIX: EQUIVALENT-PHOTON METHOD

The equivalent-photon method is a useful technique for obtaining the leading high-energy behavior of electroproduction cross sections in which the scattered electron is either undetected or detected only if it is scattered into small forward angles. This technique, which traces back to early works by Fermi, Weizsäcker and Williams, and Landau and Lifshitz,¹⁵ gives the general connection between electroproduction and photoproduction cross sections. A corresponding treatment in terms of Feynman diagrams has been given by Curtis and by Dalitz and Yennie.¹⁶ We shall briefly review the formulas required for our application here.

Let us take, as an example, the production of the state X in e - p collisions. Then the electroproduction cross section integrated over the final-electron phase space can be written as

$$d\sigma_{ep \rightarrow eX} = \frac{\alpha}{2\pi^2} \int \frac{d^3p'}{EE'} \frac{g_{\mu\nu}}{k^2} \frac{g_{\alpha\beta}}{k^2} \times (2p^\mu p^\alpha + \frac{1}{2} k^2 g^{\mu\alpha}) \frac{1}{4} M^{\nu\dagger} M^\beta d\tilde{\Gamma}, \quad (A1)$$

$$d\tilde{\Gamma} = (2\pi)^4 \delta(k+P-p_X) d\Gamma,$$

where p , p' are the initial and final electron mo-

menta, P the proton momentum, p_X the total momentum of the state X , and $d\Gamma$ is the invariant phase space for the state X . In this and following formulas we ignore the electron mass m_e whenever it is safe. For $k^2 = (p-p')^2 \rightarrow 0$ we can identify

$$\lim_{k^2 \rightarrow 0} (-\frac{1}{4} M^\dagger_\mu M^\mu d\tilde{\Gamma}) = 2\omega d\sigma_{\gamma p \rightarrow X}, \quad (A2)$$

where $d\sigma_{\gamma p \rightarrow X}$ is the corresponding photoproduction cross section for real unpolarized photons of energy ω directed along the electron beam direction.

It is convenient to perform the photon polarization sums in the radiation (Coulomb) gauge. Thus we shall make the following substitution in (A1):

$$\frac{g_{\alpha\beta}}{k^2} \rightarrow \frac{-g_{0\alpha} g_{0\beta}}{k^2} - \sum_{i=1,2} \frac{g_{i\alpha} g_{i\beta}}{k^2}. \quad (A3)$$

The polarization directions i are orthogonal to \hat{k} . The contribution of the transverse-current terms to (A1) is

$$\frac{\alpha}{2\pi^2} \int \frac{d^3p'}{EE'} \left(\frac{1}{k^2}\right)^2 \frac{1}{4} \sum_{i,j=1,2} M_i^\dagger M_j d\tilde{\Gamma} \left(-\frac{1}{2} k^2 \delta_{ij} + 2p_i p_j\right), \quad (A4)$$

which becomes

$$\frac{\alpha}{2\pi^2} \int \frac{d^3p'}{EE'} \left(\frac{1}{k^2}\right)^2 \frac{1}{4} \sum_{j=1,2} |M_j|^2 d\tilde{\Gamma} \left(-\frac{1}{2} k^2 + \frac{E^2 E'^2}{k^2} \sin^2 \theta'\right), \quad (A5)$$

when averaged over the azimuthal angle φ' of \vec{p}' where $\cos \theta' = \hat{p} \cdot \hat{p}'$. If we approximate $\frac{1}{4} \sum_j |M_j|^2 d\tilde{\Gamma}$ by its value (A2) on the photon mass shell ($k^2=0$) and ignore the longitudinal contribution, then we obtain the equivalent-photon-approximation result

$$d\sigma_{ep \rightarrow eX}^{(0)} = \int_0^E \frac{d\omega}{\omega} N(\omega) d\sigma_{\gamma p \rightarrow X}(\omega), \quad (A6)$$

where $\omega = E - E'$ and

$$N(\omega) = \frac{\alpha}{2\pi^2} (2\pi) \int_{-1}^1 d\cos \theta' \frac{2\omega^2 E'}{E} \left(\frac{1}{k^2}\right)^2 \left(-\frac{1}{2} k^2 + \frac{E^2 E'^2}{k^2} \sin^2 \theta'\right) = \frac{\alpha}{\pi} \left[\frac{E^2 + E'^2}{E^2} \left(\ln \frac{E}{m_e} - \frac{1}{2}\right) + \frac{(E-E')^2}{2E^2} \left(\ln \frac{2E'}{E-E'} + 1\right) + \frac{(E+E')^2}{2E^2} \ln \frac{2E'}{E+E'} \right] \quad (A7)$$

in the limit $m_e \ll E$. The origin of the leading $\ln(E/m_e)$ contribution is the logarithmic dependence of the θ' integration near $\theta' \sim 0$, where

$$-k^2 \approx 2EE'(1 - \cos \theta') + \frac{m_e^2 (E-E')^2}{EE'}. \quad (A8)$$

Note that the leading $\ln(E/m_e)$ contribution arises only from (A6) and not from the Coulomb excitation (scalar photon) term or the remainder terms of the transverse cross section which are not singular at $k^2=0$. Therefore, unless the Coulomb excitation current is anomalously large or the transverse cross section has an anomalous dependence on k^2 , the equivalent-photon contribution dominates for $\ln(E/m_e) \gg 1$.

Although we have found the Coulomb gauge the most convenient for our purpose, the same result can of course be obtained in any gauge.

*Work supported in part by the National Science Foundation and in part by the U. S. Atomic Energy Commission.

†Present address: The Rockefeller University, New York, N. Y. 10021.

¹In the two-photon processes the incident particles participate only as the suppliers of photons. Thus, it is irrelevant whether they are electrons or positrons. For simplicity we shall call them both electrons throughout this paper unless specified otherwise.

²S. J. Brodsky, T. Kinoshita, and H. Terazawa, *Phys. Rev. Letters* **25**, 972 (1970).

³N. Arteaga-Romero, A. Jaccarini, and P. Kessler, *Compt. Rend.* **B269**, 153 (1969); **B269**, 1129 (1969); N. Arteaga-Romero, A. Jaccarini, P. Kessler, and J. Parisi, *Lett. Nuovo Cimento* **4**, 933 (1970); *Phys. Rev. D* **3**, 1569 (1971).

⁴V. E. Balakin, V. M. Budnev, and I. F. Ginsburg, *Zh. Eksperim. i Teor. Fiz. Pis'ma v Redaktsiyu* **11**, 559 (1970) [*Soviet Phys. JETP Letters* **11**, 388 (1970)]; V. M. Budnev and I. F. Ginsburg, *Novosibirsk Report No. TP-55*, 1970 (unpublished).

⁵J. D. Bjorken, *Phys. Rev.* **148**, 1467 (1966); V. N. Gribov, B. L. Ioffe, and I. Ya. Pomeranchuk, *Phys. Letters* **24B**, 554 (1967). As for theoretical studies of the one-photon annihilation mechanism, see especially N. Cabibbo and R. Gatto, *Phys. Rev.* **124**, 1577 (1961).

⁶H. Cheng and T. T. Wu, *Phys. Rev. Letters* **23**, 1311 (1969); *Phys. Rev. D* **1**, 2775 (1970), and references therein.

⁷This cross-over energy is somewhat higher than that of Ref. 2. This is because we have used here an exact formula for $\sigma_{\gamma\gamma \rightarrow \pi^+ \pi^-}$ [see (5.5)], whereas we approximated it in Ref. 2 by ignoring the term of order m_π^2/s .

⁸Our work was stimulated especially by the report of large cross sections for hadron production for $1.6 \leq 2E \leq 2.0$ GeV reported by the experimental groups at Frascati. See Ref. 13.

⁹E. J. Williams, *Kgl. Danske Videnskab. Selskab, Mat.-Fys. Medd.* **13** (No. 4), (1934); L. Landau and E. Lifshitz, *Physik Z. Sowjetunion* **6**, 244 (1934).

¹⁰See W. C. Barber, B. Gittelman, G. K. O'Neill, and B. Richter, *Phys. Rev. Letters* **16**, 24, 1127 (1966), and references therein.

¹¹F. Calogero and C. Zemach, *Phys. Rev.* **120**, 1860 (1960).

¹²F. E. Low, *Phys. Rev.* **120**, 582 (1960). Notice that there is a misprint in the expression for $f(x)$ [Eq. (3)] in this paper.

¹³B. Bartoli *et al.*, G. Barbiellini *et al.*, V. Alles-Borelli *et al.*, and R. Baldini-Celio *et al.*, reports submitted to the Fifteenth International Conference on High-Energy Physics, Kiev, U.S.S.R., 1970 (unpublished).

¹⁴P. C. DeCelles and J. F. Goehl, Jr., *Phys. Rev.* **184**, 1617 (1969).

¹⁵E. Fermi, *Z. Physik* **29**, 315 (1924); C. Weizsäcker and E. J. Williams, *ibid.* **88**, 612 (1934); L. Landau and E. Lifshitz, *Physik Z. Sowjetunion* **6**, 244 (1934).

¹⁶R. B. Curtis, *Phys. Rev.* **104**, 211 (1956); R. H. Dalitz and D. R. Yennie, *ibid.* **105**, 1598 (1957).

¹⁷S. J. Brodsky, T. Kinoshita, and H. Terazawa, *Phys. Rev. Letters* **27**, 280 (1971). The general idea of this paper was presented by one of us (S. J. B.) at the APS Annual Meeting at New York, 1971 (unpublished).

¹⁸ $q = |q|$ or $-|q|$ depending on $d\Gamma$.

¹⁹See also J. Parisi, *Thèse de troisième cycle*, Paris, 1970 (unpublished).

²⁰Particle Data Group, *Phys. Letters* **33B**, 1 (1970).

²¹Another possible explanation of this discrepancy, which cannot be dismissed at present, is that, whereas the leading $[\ln(E/m_e)]^2$ term is given correctly by the equivalent-photon method, the exact cross section contains a contribution linear in $\ln(E/m_e)$ with a large coefficient, e.g., $[\ln(E/m_\pi)]^2$, which cannot be evaluated by the equivalent-photon method. Although we have some preliminary results supporting this interpretation, further careful analysis will be needed before we can draw a firm conclusion.

²²A. I. Akhiezer and V. B. Berestetskii, *Quantum Electrodynamics* (Interscience, New York, 1965), p. 450.

²³This result is larger by a factor of $\frac{3}{2}$ than the result of Ref. 22, pp. 454 and 484.

²⁴See Ref. 22. Our expression (5.5) is smaller by a factor of 2 than that in this reference [Eq. (60.7), p.844].

²⁵This result supersedes formula (1) of Ref. 2 which is too large by a factor of $\frac{3}{2}$ because of omission of terms of order m_π^2/s .

²⁶See Ref. 22, p. 843.

²⁷See Ref. 22, p. 450.

²⁸We wish to thank Ronald Madaras for calling our attention to errors in Tables IV and V and Figs. 15–18 in the preliminary version of this paper.

²⁹D. H. Lyth, University of Lancaster report, 1970 (unpublished). This paper treats $\pi^0\pi^0$ production in addition to $\pi^+\pi^-$ production.

³⁰A. Q. Sarker, *Phys. Rev. Letters* **25**, 1527 (1970).

³¹H. D. I. Abarbanel and M. L. Goldberger, *Phys. Rev.* **165**, 1594 (1968).

³²J. T. Manassah and S. Matsuda, *Phys. Rev. D* **3**, 882 (1971).

³³We wish to thank G. Grammer for computing the case $\theta_1 = 5.7^\circ$, $\theta_2 = 174.3^\circ$.

³⁴See, e.g., G. Bonneau and F. Martin, Orsay report, 1971 (unpublished); Z. Kurst, R. Muradyan, V. M. Ter-Antonyan, *Dubna Report No. E2-5347*, 1970 (unpublished); and A. M. Litke, Ph. D. thesis (Harvard University, 1970) (unpublished).

³⁵J. J. Sakurai, report presented to the Fifteenth International Conference on High-Energy Physics, Kiev, U.S.S.R., 1970 (unpublished).

³⁶V. G. Servo, *Zh. Eksperim. i Teor. Fiz. Pis'ma v Redaktsiyu* **12**, 50 (1970) [*Soviet Phys. JETP Letters* **12**, 39 (1970)].

³⁷Methods for measuring the photon-photon total cross sections by the Primakoff effect have recently been discussed by L. Stodolsky, *Phys. Rev. Letters* **26**, 404 (1971); N. Jurisic and L. Stodolsky, *Phys. Rev. D* **3**, 724 (1971).

³⁸Aviv, Hari Dass, and Sawyer have recently calculated the *soft-pion* cross section for $\gamma + \gamma \rightarrow \pi^+ + \pi^- + \pi^0$ making use of the Adler anomalies. Their result is too small [$\sim 10^{-35}$ cm² for $s = (4m_\pi)^2$] to generate a large enough cross section for $e + e \rightarrow e + e + \pi^+ + \pi^- + \pi^0$. R. Aviv, N. D. Hari Dass, and R. F. Sawyer, *Phys. Rev. Letters* **26**, 591 (1971). See also J. Rosner and R. Goble, University of Minnesota report, 1971 (unpublished).

³⁹One of us (H. T.) has estimated the magnitude of cross sections for $\gamma + \gamma \rightarrow \pi^+ + \pi^-$, $2\pi^+ + 2\pi^-$, $3\pi^+ + 3\pi^-$, ..., using the *soft-pion* technique with PCAC and the algebra of currents. The *soft-pion* cross section for $e + e \rightarrow e + e + \pi^+ + \pi^-$ is very close to the Born cross sections for $E = 1$ GeV. Also the ratio of the *soft-pion* cross sections

for $e+e \rightarrow e+e+2\pi^+ + 2\pi^-$ and $e+e \rightarrow e+e+ \pi^+ + \pi^-$ is 0.003 for $E=1$ GeV. The results will be found in H. Terazawa, Phys. Rev. Letters 26, 1207 (1971).

⁴⁰For the case in which both electrons are detected see Refs. 3 and 4 and also R. W. Brown and I. J. Muzinich, this issue, Phys. Rev. D 4, 1497 (1971).

⁴¹J. Parisi and P. Kessler, Collège de France, Paris report, 1970 (unpublished). This paper treats the process $e+e \rightarrow e+e+\pi^0$ in which one of the electrons is scattered into a large angle.

⁴²J. D. Bjorken, Phys. Rev. 179, 1547 (1969).

⁴³This cross section is not included in the present measurements of the pp total cross section based on the transmission technique which requires deflection of incident beam into angles much larger than the typical angles involving electron-positron pair production by the two-photon mechanism.

⁴⁴S. D. Drell and T. M. Yan, Phys. Rev. Letters 25, 316 (1970). See also G. Altarelli, R. A. Brandt, and

G. Preparata, *ibid.* 26, 42 (1971).

⁴⁵J. H. Christenson, G. S. Hicks, L. M. Lederman, P. J. Limon, and B. G. Pope, Phys. Rev. Letters 25, 1523 (1970).

⁴⁶E. D. Bloom *et al.*, Phys. Rev. Letters 23, 930 (1969).

⁴⁷S. J. Brodsky and S. C. C. Ting, Phys. Rev. 145, 1018 (1966).

⁴⁸L. H. Chan, L. Clavelli, and R. Torgerson, Phys. Rev. 185, 1754 (1969). See also A. Baracca and A. Bramon, Nuovo Cimento 51A, 873 (1967) and references therein.

⁴⁹Invited talk by G. Salvini at the APS Spring Meeting in Washington, D. C., 1971 (unpublished). The cross sections for the production of $\pi^+ \pi^-$ plus neutral particles and of more than four charged particles plus neutral ones are reported to be $(10 \pm 5) \times 10^{-33}$ cm² and $(5 \pm 3) \times 10^{-33}$ cm², respectively. We have taken these values as the upper limits for the products of the two-photon cross section for η' production and the branching ratios of respective decay modes of η' .